NASA
Technical
Paper
2937

February 1990

Integrated Force Method Versus Displacement Method for Finite Element Analysis

Surya N. Patnaik,
Laszlo Berke, and
Richard H. Gallagher

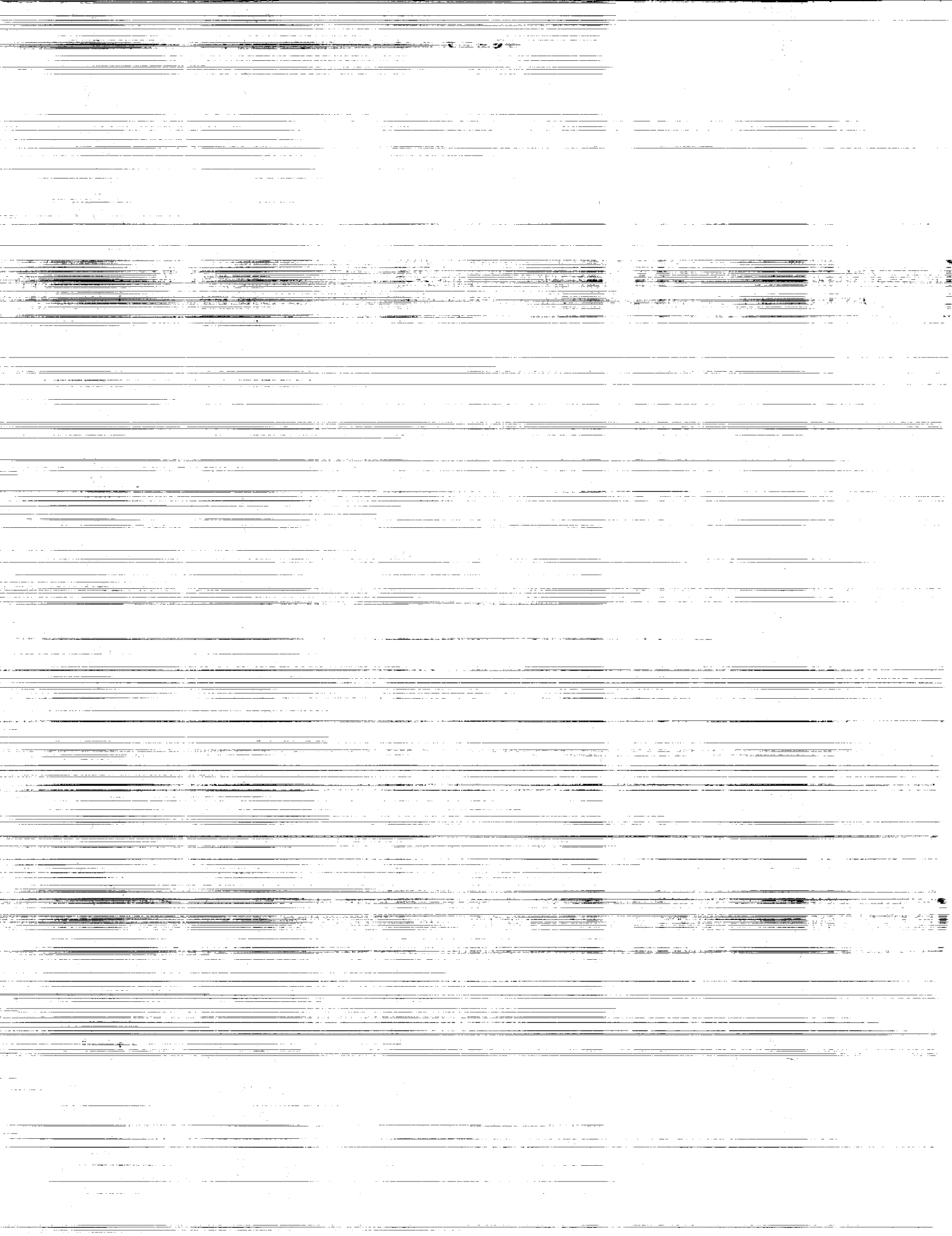

NASA Technical Paper 2937

1990

Integrated Force Method Versus Displacement Method for Finite Element Analysis

Surya N. Patnaik
and Laszlo Berke
Lewis Research Center
Cleveland, Ohio

Richard H. Gallagher
Clarkson University
Potsdam, New York

National Aeronautics and Space Administration
Office of Management
Scientific and Technical Information Division

Summary

A novel formulation termed the "integrated force method" (IFM) has been developed in recent years for analyzing structures. In this method all the internal forces are taken as independent variables, and the system equilibrium equations (EE's) are integrated with the global compatibility conditions (CC's) to form the governing set of equations. In IFM the CC's are obtained from the strain formulation of St. Venant, and no choices of redundant load systems have to be made, in contrast to the standard force method (SFM). This property of IFM allows the generation of the governing equation to be automated straightforwardly, as it is in the popular stiffness method (SM). In this report IFM and SM are compared relative to the structure of their respective equations, their conditioning, required solution methods, overall computational requirements, and convergence properties as these factors influence the accuracy of the results. Overall this new version of the force method produces more accurate results than the stiffness method for comparable computational cost.

Introduction

Solutions of structural mechanics problems must satisfy the appropriate equilibrium equations (EE's) and compatibility conditions (CC's) in addition to the constitutive relations (CR's) describing material behavior. In what order, and to what extent, these three requirements are satisfied defines the method of analysis and the quality of the solution. This report concentrates on the relative roles of EE's and CC's in structural analysis. The constitutive relations, combinations of proper mathematical models and experimental results, here are presumed to be available in valid forms, even though that is not always the case.

This report compares the two most fundamental approaches to analyzing finite element models of structures: the force method and the displacement method. The details of these two methods, and their relative characteristics, were discussed intensively three decades ago during the early evolution of computer-automated structural analysis. As is well known, the displacement method won out for computer automation in the form of the stiffness method (SM). As briefly discussed herein, the force method available at that time was based on the concept of redundant selections. It was the result of approaches developed for hand calculation in the precomputer era and proved inconvenient to automate and computationally more costly than the displacement method.

A new version of the force method, described herein and compared with the displacement method, was introduced in references 1 and 2 and termed "the integrated force method" (IFM). It is shown in a comparison with the early force methods (ref. 1) that the IFM makes automation as convenient as it is with the displacement method and yet retains the known potential for superior stress-field accuracy of finite element models that is associated with force method solution techniques. Furthermore IFM provides a convenient way to enforce an additional constraint on a finite element model of a continuum, namely strain compatibility at the interelement boundaries. This constraint, usually not satisfied, appears to result in significant improvement in accuracy.

The IFM integrates the system EE's and the global CC's in a fashion paralleling approaches in continuum mechanics (e.g., the Beltrami-Michell formulation of elasticity (ref. 3)). The IFM is a natural way of integrating the use of EE's and CC's. In contrast, the classical force method (refs. 4 and 5) (referred to in this report as "the standard force method" (SFM)), satisfies the CC's through the somewhat ad hoc and artificial concept of selected redundant internal forces. Consequently, IFM provides a strong motivation to reexamine the relative merits of the force and displacement methods within the context of the finite element idealization. A project was begun for that purpose, and its results are presented in this report.

The primary conclusions of the comparison are as follows:

(1) The IFM inherits from the SFM the ability to operate directly on stress parameters and thus to provide potentially more accurate stress results than does the displacement method.

(2) The IFM equations for finite element discrete analysis form a well-conditioned system.

(3) Discrete analysis solutions (stresses and displacements) obtained by IFM tend to converge to correct solutions more rapidly, in terms of the number of elements, than the same solution generated by the stiffness method.

(4) Examples indicate that certain problems can be solved by IFM in less computation time than by SM.

(5) Initial deformation problems are more elegantly treated by IFM than by SM.

This research indicated that with further development the IFM can become a robust and versatile analysis formulation and a viable alternative to the popular displacement method. The nature of its equations makes the IFM an attractive candidate

for the inclusion of initial deformations from various sources (e.g., manufacturing tolerances or significant thermal effects and material nonlinearities).

Historical Background

It is of some interest to briefly revisit the historical evolution of the various formulations for solving structural mechanics problems, and specifically that of the displacement and force methods.

The concepts of equilibrium of forces and compatibility of deformations are fundamental to analysis methods for solving problems in structural mechanics. There was a certain degree of asymmetry in the development and utilization of these two concepts, as described here.

Early on, when hand calculations were used, the force method was favored because it resulted in a much smaller set of simultaneous equations, usually related to the redundant forces in a roof or bridge truss, than did the displacement method. With the appearance of computers that consideration lost its importance in favor of ease of automation and low computational cost.

Equilibrium can be viewed as a more fundamental concept than compatibility. Engineers have a feel for it, perhaps because it was practiced consciously or subconsciously by the first builders of primitive human habitats in the dim past of human evolution, by the architects of magnificent edifices of biblical empires, and then by the builders of cathedrals, who faced the intricate equilibrium problems of Roman and Gothic arches and domes. If equilibrium was violated, or was precarious, the construction responded by tumbling down. Recall that the mere blast of horns is supposed to have caused certain walls in Jericho to collapse in a much simpler era of structural analysis and construction practices.

The point is that equilibrium is such a natural concept that good engineers have always had a feel for it, and it was the guidance for most early achievements. In contrast, the more sophisticated and basically mathematical concept of compatibility certainly was not central to the worries of these early builders and architects; it was not even known until mathematicians defined it only a century ago.

Rational principles to define the equilibrium conditions of mechanical forces had an early start with the work of Archimedes (287–212 B.C.) on levers and pulleys. A couple of millennia passed before the upsurge of rational scientific thought during the Renaissance brought about further significant theoretical developments. With the efforts of many scientists during the centuries that followed, the concepts of equilibrium and compatibility were finally developed in forms that eventually became useful for design calculations. Because it helps to understand how the current computer-automated analysis practices evolved, the history of this development is briefly reviewed.

Renaissance geniuses like Leonardo da Vinci (1452–1519) and Gallileo (1564–1642) used the concept of equilibrium in their work, but even Gallileo, a professor of mathematics, did not possess the proper mathematical language to express the fundamental laws governing equilibrium in a continuum. That had to wait until the introduction of that language (i.e., calculus) by Newton (1642–1726) and Leibnitz (1636–1716). This new mathematical tool attracted many of the great minds of the Age of Enlightenment, who finally were in the possession of mathematical language to formulate correct laws of physics. Elasticity was introduced as a branch of mathematics, rich in the possible applications of the exciting new tool of calculus. The Bernoulli brothers and Euler were enthusiastic early proponents of the use of calculus in mechanics. Following in their footsteps many great scientists contributed to the early developments in elasticity. A fundamental contribution was made by Cauchy (1789–1857), who formulated the equilibrium equations both in the field and on the boundary for deformable bodies (refs. 3 and 6).

The underlying principle behind the EE's is force balance, which can be easily visualized. Equilibrium equations in general are not sufficient to solve a structural analysis problem; they have to be augmented by the compatibility conditions. In other words, EE's are indeterminate in nature, and determinancy for a continuum is achieved by adding the compatibility conditions to them.

The compatibility conditions in the field (which are the counterpart of Cauchy's field equilibrium equations) were formulated in terms of strains for deformable solids by St. Venant (ref. 3) in 1864, decades after Cauchy's equilibrium formulation. Again it took about three decades for the field CC's of St. Venant to be expressed in terms of stresses by Beltrami and Michell in 1900 (ref. 6).

The CC's on the boundary, which are the counterpart of Cauchy's stress boundary conditions and are henceforth referred to as "the boundary compatibility conditions" (BCC's), eluded analysts until their recent formulation in 1986 (ref. 7). In contemporary elasticity, boundary indeterminancy is alleviated by using additional displacement boundary conditions (imposed on a kinematically stable structure) instead of the legitimate BCC's. For discrete structures the CC's were formulated in a way that would not be equivalent to the elasticity theory for a continuum (the strain formulation of St. Venant).

The development of analysis methods for discrete structures was also accelerating during the nineteenth century for practical reasons. The upsurge in scientific discoveries during the previous centuries was closely followed by their exploitation for inventions and large-scale industrialization. The need to qualitatively predict the behavior of various machinery and constructions became a driving force for the development of analytical methods.

One of the central problems was to analyze trusses and frames employed in bridges and buildings. Wooden trusses had been used since ancient times, and wooden bridges reached

spans of over 300 ft by the end of the nineteenth century. The first book on the analysis of bridge trusses was published in 1847 by Whipple (ref. 8), who had impressive wooden bridges to his credit. When iron became available in sufficient quantity to construct iron bridges of various designs, accurate methods of calculating forces were needed in order to size structural members.

The concepts of statically determinate and indeterminate structures were introduced. Equilibrium equations written at joints in terms of forces are sufficient only to calculate or graphically obtain member forces for statically determinate trusses. Two theoretical approaches (the force method and the displacement method) were developed for indeterminate structures in the second half of the nineteenth century. These are the foundations of the analytical methods used today.

For an indeterminate truss there are more force unknowns than equations, thus the indeterminancy. Clebsch (1833–1872) noticed that, if EE's are written in terms of nodal displacements, the number of equations and displacement unknowns is identical. With that observation the displacement method was born, but it was not useful because there was no practical way to solve the potentially large number of simultaneous equations by hand, except perhaps by relaxation methods, such as moment distribution introduced by Hardy Cross in the 1930's.

A more useful method was introduced by Maxwell (1831–1879), who proposed cutting redundant members and introducing unknown redundant forces at the cuts. The remaining determinate structure is solved for both applied and redundant loads in order to obtain the internal forces and the relative displacements at the cuts for all the load systems. Because the EE's for determinate trusses essentially represent a triangular system of equations, their solution is easily obtained even by hand calculations (refer to appendix A). Next, in order to reestablish discretized compatibility, the analyst sets up simultaneous equations that express the conditions at which the relative displacements due to the external loads are closed by the redundant loads. The solution of these equations yields the redundant forces, and superposition of the two sets of internal loads gives the final solution. This cumbersome method is known as the force method and referred to as "the standard force method" (SFM) in this report. This method became the analysis method of choice for generations of engineers because in conventional trusses and rigid frames the number of redundant forces, and therefore the number of simultaneous equations, was usually small—an overriding consideration before the dawn of the computer age.

One can make the observation at this point that both the force and displacement methods centered around EE's. Global compatibility was not dealt with at a similar conscious level because it is automatically satisfied in the displacement method and used only as an ad hoc device to augment the number of EE's in the preceding formulation of the force method. Otherwise no parallel approach was developed that would satisfy the system EE's and global CC's simultaneously without recourse to the concept of redundant selection.

General Description of Integrated Force Method

All numerical solutions are approximate depending on the degree to which the EE's and CC's are satisfied or violated. It is a common observation that stress fields obtained by the heavily equilibrium-based finite element stiffness method (SM) in general satisfy neither the EE's nor the CC's in regions of stress concentrations or on the interelement boundaries (ref. 9). Of course SM provides solutions of acceptable accuracy to many complex problems that could hardly be analyzed only a couple of decades ago, the accuracy being dependent mostly on the choice of the finite element model. As will be shown, this accuracy and the efficiency of computation can be greatly improved by a more direct satisfaction of EE's and CC's. Recent research on CC's led to the establishment of the novel formulation termed "the integrated force method of analysis" (refs. 1, 2, 7, and 10 to 16). The IFM explicitly constrains the primary variables (which are the forces for discrete systems and the stress resultants for continua) to satisfy both EE's and CC's within an element and at nodes and, in addition, the CC's on the interelement boundaries. The IFM thereby ensures the improved accuracy of the stress fields. Interelement equilibrium conditions, in general, are the only conditions not explicitly imposed by the IFM. The IFM has now been established for static, stability, and dynamic analyses of discrete systems and continua. The basic theory of IFM has been completed with the formulation of the variational functional for IFM (ref. 7). The stationary condition of the IFM variational functional yields all the known equations of structural mechanics along with the novel conditions identified as the boundary compatibility conditions.

The IFM for discrete analysis, similar to SM, is independent of the concept of redundants and the basis determinate structure selection of the classical force method, referred to earlier as "the standard force method" (SFM) (ref. 1). The IFM for continuum analysis is based on EE's and CC's in the field and on the boundary. Contemporary analytical methods (continua or their discrete counterparts) irrespective of analysis methodology (SFM or SM) totally exclude the consideration of the boundary compatibility requirements because the BCC's were not known. The IFM utilizes the BCC's in analysis (refs. 7, 15, and 16). Reference 1 compares the IFM to the SFM (ref. 1) and shows that the SFM developed for hand computation is a special version of the integrated force method. The SFM can be considered as a subset of the IFM, limited to static stress analysis.

In this report the integrated force method is compared with the stiffness method. The methods are compared analytically

and numerically for finite element systems taking into consideration the following five criteria:

(1) Computer automation
(2) Solution accuracy
(3) Stability of equation systems
(4) Computational efforts
(5) Versatility of methods

As the IFM is of recent origin and only research-level software implementation exists, the comparison is restricted mostly to basic principles of the formulations. Simple numerical illustrations are included to clarify issues and to show relative performances. The basic difference between the IFM and SFM solution techniques is illustrated in appendix A for simple examples.

Equations of Integrated Force Method

Generation of IFM Equations

The basic IFM equations introduced earlier (refs. 1 and 2) are presented here for completeness and for comparison with the SM equations.* A discrete or discretized structure for analysis can be designated as structure (n,m) where "structure" denotes type of structure (truss, frame, plate, shell, or their combination discretized by finite elements) and n,m are force and displacement degrees of freedoms (fof, dof), respectively. The structure (n,m) has m equilibrium equations and $r = (n-m)$ compatibility conditions. The m equilibrium equations

$$[B]\ \{F\} = \{P\}$$

and the r compatibility conditions

$$[C][G]\ \{F\} = \{\delta R\}$$

are coupled to obtain the governing equations of the IFM as

$$\begin{bmatrix} [B] \\ \hline [C][G] \end{bmatrix} \{F\} = \begin{bmatrix} P \\ \hline \delta R \end{bmatrix} \quad \text{or } [S]\{F\} = \{P\}^* \qquad (1)$$

where [B] is the $(m \times n)$ equilibrium matrix, [C] is the $(r \times n)$ compatibility matrix, [G] is the $(n \times n)$ concatenated flexibility matrix, $\{P\}$ is the m-component load vector, $\{\delta R\}$ is the r-component effective initial deformation vector,

$$\{\delta R\} = -[C]\ \{\beta\}_0$$

where $\{\beta\}_0$ is the n-component initial deformation vector, and [S] is the $(n \times n)$ IFM governing matrix. The matrices [B],[C],[G], and [S] are banded and they have full-row ranks of m, r, n, and n, respectively.

*All symbols are defined in appendix B.

The solution of equation (1) yields the n forces $\{F\}$. The m displacements $\{X\}$ are obtained from the forces $\{F\}$ by backsubstitution (ref. 1):

$$\{X\} = [J]\ \{[G]\ \{F\} + \{\beta\}_0\} \qquad (2a)$$

where [J] is the $(m \times n)$ deformation coefficient matrix defined as

$$[J] = m \text{ rows of } [[S]^{-1}]^T \qquad (2b)$$

Equations (1) and (2) represent the two key IFM relations for finite element analysis. The key equation of the stiffness method, expressing nodal equilibrium in terms of nodal displacement, has the following form:

$$[K]\ \{X\} = \{P\} + \{P\}^i \qquad (3)$$

where [K] is the $(m \times m)$ stiffness matrix and $\{P\}^i$ represents equivalent loads caused by initial imperfections.

From the IFM equations (eqs. (1) and (2)) and the stiffness method equation (eq. (3)) the following observations can be made:

(1) In IFM the internal forces $\{F\}$ are calculated directly from the applied loads $\{P\}^*$. In SM one has to calculate displacements first from loads (by using the load-displacement relation $[K]\ \{X\} = \{P\}$, noting that loads and displacements have different dimensions and magnitudes) irrespective of the analysis requirements and then determine internal forces from displacements by backsubstitution, coordinate transformations, and differentiation or its equivalent.

(2) The right-side vector $\{P\}^*$ of dimension n in IFM equation (1) is constructed from the m-component mechanical loads $\{P\}$ and the r-component effective initial deformations $\{\delta R\}$. The right-side vector of dimension m in SM includes both mechanical load vector $\{P\}$ of dimension m and m-component equivalent load vector $\{P\}^i$. The IFM load vector $\{P\}^*$ is independent of the material characteristics and design parameters of the structure. The total SM load vector is a function of the material properties and design variables of the structure. The SM equivalent loads $\{P\}^i$ are nonzero even for compatible initial deformations that do not induce stresses in the structure. In other words the problem of initial deformations in the stiffness method is handled by the concept of equivalent loads that are nonzero even for a trivial situation of compatible initial deformation distribution when $\{\delta R\} = \{0\}$.

(3) The IFM equation (eq. (1)) contains both EE's and CC's. The stiffness equation (eq. (3)) can be obtained from equation (1) by transforming variables and backsubstituting. Since equation (3) does not explicitly include the CC's, these equations cannot be manipulated to obtain IFM equations.

The steps required to obtain the stiffness equation (eq. (3)) from the IFM equation (eq. (1)) are as follows (the derivation is for mechanical loads only):

(1) Displacements are changed to deformations by using deformation displacement relations (DDR's):

$$\{\beta\} = [B]^T\{X\} \tag{4}$$

(2) Deformations are then transformed to forces by using the deformation force relation

$$\{\beta\} = [G]\{F\} \tag{5}$$

(3) Force displacement relations are obtained from equations (4) and (5) as

$$\{F\} = [G]^{-1}[B]^T\{X\} \tag{6}$$

(4) The upper portion of the EE of the IFM governing equation (eq. (1), [B] {F} = {P}) is rewritten in displacements to obtain the stiffness equation

$$[[B][G]^{-1}[B]^T]\ \{X\} = \{P\} \tag{7}$$

or [K] {X} = {P}, where $[K] = [B][G]^{-1}[B]^T$. As mentioned earlier the integrated force method cannot be obtained from the stiffness formulation owing to the explicit absence of CC's in that formulation.

IFM Solution Procedure

The IFM solution procedure is illustrated in appendix A for the example of a bar subjected to both mechanical and thermal loads. The prinicipal steps are as follows:

Step 1: Assembly of the system equilibrium matrix [B].

The system EE matrix [B] is assembled from elemental equilibrium matrices by standard finite element techniques. The procedure to generate the elemental equilibrium matrix is presented in the section "Equilibrium Equations" of this report.

Step 2: Generation of the global compatibility matrix [C].

The generation of the global compatibility matrix is presented in the section "Compatibility Conditions." Since the deformation displacement relation (eq. (4)) utilizes the EE matrix [B] and the CC's are obtained from the DDR's, accuracies or errors in the equilibrium matrix are likely to be reflected in the compatibility matrix [C].

Step 3: Generation of the concatenated flexibility matrix [G].

The block diagonal flexibility matrix [G] is obtained as the diagonal concatenation of elemental flexibility matrices. The elemental flexibility matrices are obtained by discretizing complementary strain energy functionals according to standard flexibility techniques.

Step 4: Construction of load vector $\{P\}^*$.

The IFM load vector $\{P\}^*$ is assembled from mechanical loads {P} and initial deformations $\{\beta\}_0$ as defined in equation (1).

Step 5: Solution of IFM equation.

The matrix equation (1) is constructed from matrices [B], [C], and [G] and load $\{P\}^*$, and its solution yields the forces. Displacements are obtained by backsubstituting from equations (2).

Equilibrium Equations

The equilibrium equations, written in term of forces at the grid points of a finite element model, represent the vectorial summation of n internal forces {F} and m external loads {P}. The nodal EE in matrix notation gives rise to the $(m \times n)$ $(n \geq m)$-banded rectangular equilibrium matrix [B], which is independent of the material properties and design parameters of the indeterminate structure (n,m). For finite element analysis this matrix is assembled from elemental equilibrium matrices.

The elemental equilibrium matrices [B] for bar and beam elements can be obtained from the direct force balance principle (ref. 4). For continuous structures, such as plates or shells, very few equilibrium matrices are reported in the literature (refs. 17 and 18). Equilibrium matrices for the plate flexure problem are given by Przemieniecki (ref. 17) and Robinson (ref. 18). Przemieniecki generates the matrix for a rectangular element in flexure from direct application of the force balance principle at the nodes. Robinson utilizes the concept of virtual work to derive the matrix for a rectangular-plate element in flexure. The procedures of Przemieniecki and Robinson are documented in their books (refs. 17 and 18) and are not repeated here.

Energy-equivalent equilibrium matrices for finite element analysis can be obtained from the IFM variational functional (ref. 7). The procedure to be followed to generate an elemental equilibrium matrix from the IFM variational functional is illustrated next for the example of a rectangular-plate element in flexure. The portion of the IFM functional (ref. 7) that yields the equilibrium matrix [B] for a plate bending element has the following well-known form:

$$U_p = \int_D \left\{ M_x \frac{\partial^2 w}{\partial x^2} + M_y \frac{\partial^2 w}{\partial y^2} + M_{xy} \frac{\partial^2 w}{\partial x \partial y} \right\} dx\, dy \tag{8}$$

where M_x, M_y, and M_{xy} are the plate bending moments and

$$\frac{\partial^2 w}{\partial x^2}, \qquad \frac{\partial^2 w}{\partial y^2}, \qquad \frac{\partial^2 w}{\partial x \partial y}$$

represent the curvatures. The plate domain is D and the coordinates are (x,y).

By appropriate choice of force and displacement functions the energy scalar U_p can be discretized to obtain the elemental equilibrium matrix [B].

$$U_p = \{X\}^T[B]\{F\} \tag{9}$$

where the elemental displacement degrees of freedom are symbolized by {X} and the elemental force degrees of freedom by {F}.

The force fields have to satisfy two mandatory requirements:

(1) The force fields must satisfy the homogeneous equilibrium equations (here the plate bending equations in the domain).

(2) The force components F_k $(k = 1,2,\ldots,9)$ must be independent of one another. This condition ensures the kinematic stability of the element. For the rectangular plate the force field is chosen in terms of nine independent forces:

$$\langle F \rangle = \langle F_1, F_2, \ldots, F_9 \rangle$$

as

$$\left.\begin{aligned} M_x &= F_1 + F_2 x + F_3 y + F_4 xy \\ M_y &= F_5 + F_6 x + F_7 y + F_8 xy \\ M_{xy} &= F_9 \end{aligned}\right\} \qquad (10)$$

The variation of the normal moments in the field is linear, but the twisting moment is constant. The assumed moments satisfy the mandatory requirements.

The displacement field that should satisfy the continuity condition (ref. 19) is chosen in terms of 12 variables to match the three dof (transverse nodal displacement w_i and two rotations θ_{xi} and θ_{yi} per node i for the four nodes) and can be written in terms of Hermite polynomials as

$$\begin{aligned} w(x,y) = {} & H_{01}(x)H_{01}(y)X_1 + H_{01}(x)H_{11}(y)X_2 \\ & + H_{11}(x)H_{01}(y)X_3 + H_{01}(x)H_{02}(y)X_4 \\ & + H_{01}(x)H_{12}(y)X_5 + H_{11}(x)H_{02}(y)X_6 \\ & + H_{02}(x)H_{02}(y)X_7 + H_{02}(x)H_{12}(y)X_8 \\ & + H_{12}(x)H_{02}(y)X_9 + H_{02}(x)H_{01}(y)X_{10} \\ & + H_{02}(x)H_{11}(y)X_{11} + H_{12}(x)H_{01}(y)X_{12} \end{aligned} \qquad (11a)$$

In equation (11a) the Hermite polynomials are defined as

$$\left.\begin{aligned} H_{01}(x) &= \frac{x^3 - 3a^2x + 2a^3}{4a^3} \\ H_{02}(x) &= -\frac{x^3 - 3a^2x - 2a^3}{4a^3} \\ H_{11}(x) &= \frac{x^3 - ax^2 - a^2x + a^3}{4a^2} \\ H_{12}(x) &= \frac{x^3 + ax^2 - a^2x - a^3}{4a^2} \end{aligned}\right\} \qquad (11b)$$

where $X_1, X_2, \ldots, X_{12}$ are the 12 dof and a and b are the dimensions of the plate along the x and y directions, respectively. The Hermite polynomials for the y coordinate direction can be obtained by changing x and a to y and b, respectively, in equation (11b). The displacement field (eq. (11a)) gives rise to linear force distribution (eq. (10)) for the plate bending problem.

The equilibrium matrix is obtained by substituting moments from equations (10) and displacements from equations (11) into the energy scalar given by equation (8) and integration. The equilibrium matrix thus obtained is presented in table I. The generation of the equilibrium matrix [B] from the IFM functional is a general procedure applicable to any other type of element. The matrix obtained from the functional is henceforth referred to as the consistent equilibrium matrix $[B]_s$.

The two equilibrium matrices of Przemieniecki and Robinson, depicted in tables II and III, are compared with the IFM consistent matrix for response accuracy. In this study the analysis was carried out by IFM following the five steps given in the section "IFM Solution Procedure."

TABLE I.—IFM CONSISTENT EQUILIBRIUM MATRIX $[B]_s$ FOR RECTANGULAR-PLATE ENDING ELEMENT

0	b	0	$\frac{-2b^2}{5}$	0	0	a	$\frac{-2a^2}{5}$	-2
0	$\frac{b^2}{3}$	0	$\frac{-b^3}{15}$	$-a$	$\frac{2a^2}{5}$	ab	$\frac{-2a^2b}{5}$	0
b	$-ab$	$\frac{-2b^2}{5}$	$\frac{2ab^2}{5}$	0	0	$\frac{-a^2}{3}$	$\frac{a^3}{15}$	0
0	b	0	$\frac{2b^2}{5}$	0	0	$-a$	$\frac{2a^2}{5}$	2
0	$\frac{-b^2}{3}$	0	$\frac{-b^3}{15}$	a	$\frac{-2a^2}{5}$	ab	$\frac{-2a^2b}{5}$	0
$-b$	$-ab$	$\frac{2b^2}{5}$	$\frac{-2ab^2}{5}$	0	0	$\frac{a^2}{3}$	$\frac{-a^3}{15}$	0
0	$-b$	0	$\frac{-2b^2}{5}$	0	0	$-a$	$\frac{-2a^2}{5}$	-2
0	$\frac{b^2}{3}$	0	$\frac{b^3}{15}$	a	$\frac{2a^2}{5}$	ab	$\frac{2a^2b}{5}$	0
$-b$	$-ab$	$\frac{-2b^2}{5}$	$\frac{-2ab^2}{5}$	0	0	$\frac{-a^2}{3}$	$\frac{-a^3}{15}$	0
0	$-b$	0	$\frac{2b^2}{5}$	0	0	a	$\frac{2a^2}{5}$	2
0	$\frac{-b^2}{3}$	0	$\frac{b^3}{15}$	$-a$	$\frac{-2a^2}{5}$	ab	$\frac{2a^2b}{5}$	0
b	$-ab$	$\frac{2b^2}{5}$	$\frac{2ab^2}{5}$	0	0	$\frac{a^2}{3}$	$\frac{a^3}{15}$	0

TABLE II.—PREZEMIENIECKI'S EQUILIBRIUM MATRIX $[B]_P$ FOR RECTANGULAR-PLATE BENDING ELEMENT

[Dimension of element, (a,b).]

0	$\frac{2}{b}$	0	0	0	0	0	$\frac{-2}{a}$	−1
1	1	0	0	0	0	0	0	0
0	0	0	0	0	0	−1	1	0
0	$\frac{-2}{b}$	0	$\frac{2}{a}$	0	0	0	0	1
−1	1	0	0	0	0	0	0	0
0	0	−1	−1	0	0	0	0	0
0	0	0	$\frac{-2}{a}$	0	$\frac{2}{b}$	0	0	−1
0	0	0	0	−1	−1	0	0	0
0	0	1	−1	0	0	0	0	0
0	0	0	0	0	$\frac{-2}{b}$	0	$\frac{2}{a}$	1
0	0	0	0	1	−1	0	0	0
0	0	0	0	0	0	1	1	0

TABLE III.—ROBINSON'S EQUILIBRIUM MATRIX $[B]_R$ FOR RETANGULAR-PLATE BENDING ELEMENT

[Dimension of element, (a,b).]

0	$-b$	0	$\frac{2b^2}{5}$	0	0	$-a$	$\frac{2b^2}{5}$	2
0	$\frac{-b^2}{3}$	0	$\frac{b^3}{15}$	a	$\boxed{\frac{-a^2}{3}}$	$-ab$	$\boxed{\frac{a^2b}{3}}$	0
$-b$	ab	$\boxed{\frac{b^2}{3}}$[a]	$\boxed{\frac{-ab^2}{3}}$	0	0	$\frac{a^2}{3}$	$\frac{-a^2}{15}$	0
0	b	0	$\frac{-2b^2}{5}$	0	0	$-a$	$\frac{-2a^2}{5}$	−2
0	$\frac{b^2}{3}$	0	$\frac{-b^3}{15}$	a	$\boxed{\frac{a^2}{3}}$	$-ab$	$\boxed{\frac{-a^2b}{3}}$	0
b	ab	$\boxed{\frac{-b^2}{3}}$	$\boxed{\frac{-ab^2}{3}}$	0	0	$\frac{-a^2}{3}$	$\frac{-a^3}{15}$	0
0	b	0	$\frac{2b^2}{5}$	0	0	a	$\frac{2a^2}{5}$	2
0	$\frac{-b^2}{3}$	0	$\frac{-b^3}{15}$	$-a$	$\boxed{\frac{-a^2}{3}}$	$-ab$	$\boxed{\frac{-a^2b}{3}}$	0
b	ab	$\boxed{\frac{b^2}{3}}$	$\boxed{\frac{ab^2}{3}}$	0	0	$\frac{a^2}{3}$	$\frac{a^3}{15}$	0
0	$-b$	0	$\frac{-2b^2}{5}$	0	0	a	$\frac{-2a^2}{5}$	−2
0	$\frac{b^2}{3}$	0	$\frac{b^3}{15}$	$-a$	$\boxed{\frac{a^2}{3}}$	$-ab$	$\boxed{\frac{-a^2b}{3}}$	0
$-b$	ab	$\boxed{\frac{-b^2}{3}}$	$\boxed{\frac{ab^2}{3}}$	0	0	$\frac{-a^2}{3}$	$\frac{a^3}{15}$	0

[a]Boxed elements had coefficient changed from 1/3 in Robinson's matrix to 2/5 in IFM consistent matrix.

IFM Consistent Matrix Versus Przemieniecki's Matrix

The elemental discretizations by the IFM and Przemieniecki approaches are identical in force and displacement degrees of freedoms, with fof = 9 and dof = 12 for both. This gives rise to identical dimensions of 12 × 9 for both matrices $[B]_s$ and $[B]_P$. In the IFM approach the moment variables are in units of moment per unit length (such as kip-inch per inch or kilogram-meter per meter). Przemieniecki concentrates the moments at the nodes, and this accounts for the dimension change between the elemental matrices $[B]_s$ and $[B]_P$. The number of nonzero entries in the Przemieniecki matrix is 28. In contrast, there are 68 entries in the IFM matrix $[B]_s$. The Przemieniecki matrix can be viewed as a lumped version, whereas the IFM matrix is consistent. The quality of the response was ascertained by using both the matrices $[B]_s$ and $[B]_P$ to solve a finite element model of a clamped square plate in flexure (plate material, steel; size, 40 in. (101.6 cm); and thickness, 0.2 in. (5.08 mm)) with a concentrated load at its center (P = 1000 lb (453.59 kg)). Other analysis features in the IFM procedure, such as the flexibility matrix and compatibility generation scheme, were kept identical for both cases. The deflection at the plate center was chosen as the parameter for comparison. This parameter was obtained in IFM by first calculating forces from equation (1) and then substituting {F} in equation (2). The displacement for this problem as given by Timoshenko (ref. 20) had the following value for the plate depicted in figure 1:

$$w_c = 0.4072 \text{ in. } (10.343 \text{ mm}) \tag{12}$$

The central displacements obtained with the two matrices ($[B]_s$ and $[B]_P$) for the two finite element models are presented in table IV. Table IV shows that the central deflection obtained with the IFM matrix $[B]_s$ converged to Timoshenko's series solution for the first model with four elements. Przemieniecki's equilibrium matrix $[B]_P$ not only yielded a higher value for the central displacement w_c for the

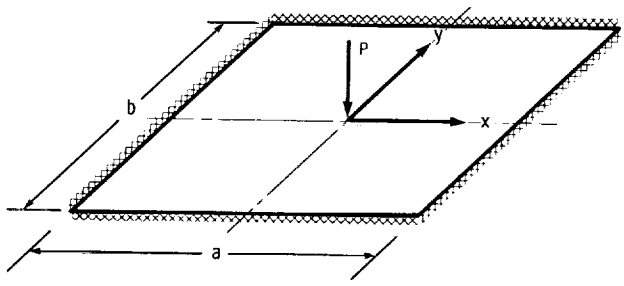

Figure 1.—Clamped plate. Along clamped edges $w = \partial w/\partial x = \partial w/\partial y = 0$.

TABLE IV.—IFM ANALYSIS RESULTS—RESPONSE BY PREZEMIENIECKI MATRIX $[B]_P$ VERSUS IFM CONSISTENT MATRIX $[B]_s$

[Timoshenko's solution, w_c = 0.4072 in. (10.343 mm).]

Number of elements	Przemieniecki matrix			IFM matrix		
	Central displacement, w_c		Error, percent	Central displacement, w_c		Error, percent
	in.	mm		in.	mm	
4	0.5054	12.8372	24.11	0.4083	10.3708	0.20
16	.5509	13.9929	35.29	.4069	10.3353	.07

four-element model, but also did not show the tendency of monotonic convergence for the refined model consisting of 16 elements.

IFM Consistent Matrix Versus Robinson's Matrix

The IFM matrix bears a remarkable resemblance to Robinson's matrix except for the following;

(1) There is a change in sign between the two matrices. The reason is that the IFM sign convention is opposite to that of Robinson's notations.

(2) Some of the elements with coefficient 1/3 in Robinson's matrix $[B]_R$ were changed to 2/5 in the IFM consistent matrix. This difference occurred for the 16 elements noted in table III. For the test example of a clamped plate, however, the discrepancy had a negligible effect on the solution for moments and displacements as shown in table V.

When element geometry becomes complicated, it is rather difficult to generate the equilibrium matrix by vectorial summation of forces (ref. 17) or by repeated use of virtual influence coefficients (ref. 18). Therefore it is recommended that the elemental equilibrium matrices should be generated by following the IFM consistent approach (ref. 7).

The equilibrium matrix $[B]_s$ corresponds to three displacement variables per node (displacement w and two rotations θ_x and θ_y), giving rise to 12 variables per node. This idealization requires a displacement polynomial with 12 unknowns. Only 12-term Hermite polynomials are used to satisfy this requirement. The 12-term Hermite polynomial is known to cause convergency difficulties in the stiffness method. The effect of the 12-term Hermite polynomial on solution accuracy in the integrated force method was examined by using a displacement function given by equation (13) to obtain another equilibrium matrix, designated as $[B]_a$. This displacement function has the following form:

$$w(x,y) = \alpha_1 + \alpha_2 x + \alpha_3 y + \alpha_4 x^2 + \alpha_5 xy + \alpha_6 y^2 + \alpha_7 x^3 + \alpha_8 x^2 y + \alpha_9 xy^2 + \alpha_{10} y^3 + \alpha_{11} x^3 y + \alpha_{12} xy^3 \qquad (13)$$

The constants of the polynomial were related to nodal dof by following standard finite element techniques, and the 12×9 equilibrium matrix $[B]_a$ was obtained from equations (8), (10), and (13). Few coefficients of the matrices $[B]_s$ and $[B]_a$ are different.

In order to examine the effect on the solution accuracy, the clamped plate was analysed by using both equilibrium matrices $[B]_s$ and $[B]_a$ along with the appropriate flexibility and compatibility matrices as described in the subsection "IFM Solution Procedure." The plate properties are defined in the main section "Solution Accuracy." The central displacements obtained for three idealizations (model 1 has 4 elements, model 2 has 16, and model 3 has 36) by using the two matrices were as follows:

(1) For EE matrix $[B]_s$. The central displacements w_c for the three idealizations were 0.2041, 0.2035, and 0.2035 in. (5.181, 5.169, and 5.169 mm), respectively.

TABLE V.—IFM ANALYSIS RESULTS—RESPONSE BY ROBINSON'S MATRIX $[B]_R$ VERSUS RESPONSE BY IFM CONSISTENT MATRIX $[B]_s$

Number of elements	Robinson's matrix				IFM matrix			
	Central displacement, w_c		Moment at plate center, $M_x = M_y$		Central displacement, w_c		Moment at plate center, $M_x = M_y$	
	in.	mm	(kip in.)/in.	(kg m)/m	in.	mm	(kip in.)/in.	(kg m/m)
4	0.4083	10.3708	0.193	87.544	0.4083	10.3708	−0.193	−87.544
16	.4069	10.3353	.241	109.317	.4069	10.3353	−.241	−109.317

(2) For EE matrix $[B]_a$. The central displacements w_c for the three idealizations were 0.2041, 0.2035, and 0.2035 in. (5.181, 5.169 and 5.169 mm), respectively.

For the problem both matrices gave identical values for the central displacement. Moments obtained for both cases were also identical.

In the stiffness method it is a known fact that the solution is sensitive to the choice of displacement fields (refer to eqs. (11) and (13)). In the IFM displacement fields do not have a significant effect on solution accuracy. For the plate problem the two different displacement fields given by equations (11) and (13) yielded identical results. This feature of IFM is further elaborated in the subsection "Element Level Effect."

Compatibility Conditions

The compatibility conditions are constraints on strains, and for finite element models they are also constraints on member deformations $\{\beta\}$. The n-component deformation vector is defined as

$$\{\beta\} = [G]\{F\} + \{\beta\}_0 \tag{14}$$

where $\{\beta\}$ is the total deformation, [G] is the flexibility matrix, {F} represents the member forces, and $\{\beta\}_0$ is the initial deformation. When expressed in terms of force variables the CC's involve two matrices, the flexibility matrix [G] and the compatibility matrix [C], and can be written as

$$[C][G]\{F\} = \{\delta R\} \tag{15}$$

This equation augments the EE's in the IFM as given in equation (1). The flexibility matrix [G] is obtained from the discretization of the complementary strain energy by following standard techniques. For the plate element example the flexibility matrix $[G]_e$ can be symbolically represented as

$$U_c = \frac{1}{2}\{F\}^T[G]_e\{F\}$$

$$= \left(\frac{D^1}{2}\right)\int\left\{M_x^2 + M_y^2 - 2\nu M_x M_y + (1+\nu)M_{xy}^2\right\} dx\, dy \tag{16}$$

where $D^1 = (Eh^3/12)$, E is Young's modulus, ν is Poisson's ratio, and h is the plate thickness.

Substituting into equation (16) the moments M_x, M_y, and M_{xy} in terms of forces F_1, F_2, ..., F_9 as given by equation (10) and integrating yield the (9 × 9) flexibility matrix $[G]_e$ for the rectangular-plate flexure element. The generation of the flexibility matrix [G] is reported in the literature (refs. 4, 17, and 18) and will not be repeated here. The system flexibility matrix [G] for the structure is a block diagonal matrix. It is obtained as the diagonal concatenation of element flexibility matrices.

Generation of Compatibility Matrix [C]

The compatibility matrix [C] is obtained by extending St. Venant's theory of elasticity strain formulation to discrete structural mechanics (refs. 11 and 12). The procedure is illustrated by taking the plane stress elasticity problem as an example. The strain displacement relations (SDR's) of the problem are

$$\left.\begin{aligned}\epsilon_x &= \frac{\partial u}{\partial x}\\ \epsilon_y &= \frac{\partial v}{\partial y}\\ \gamma_{xy} &= \frac{\partial u}{\partial y} + \frac{\partial v}{\partial x}\end{aligned}\right\} \tag{17a}$$

In the SDR's three strains (ϵ_x, ϵ_y, and γ_{xy}) are expressed as functions of two displacements (u and v). The compatibility constraint on strains is obtained by eliminating the two displacements from the three SDR's, resulting in the single compatibility condition

$$\frac{\partial^2\epsilon_x}{\partial y^2} + \frac{\partial^2\epsilon_y}{\partial x^2} - \frac{\partial^2\gamma_{xy}}{\partial x\partial y} = 0 \tag{17b}$$

The two steps of St. Venant's procedure to generate CC's are as follows:

(1) Establish the SDR's.

(2) Eliminate displacements from the SDR's to obtain the CC's.

The equivalents of SDR's in the mechanics of discrete structures are the deformation displacement relations (DDR's); deformations $\{\beta\}$ of the discrete analysis are analogous to strains $\{\epsilon\}$ of the elasticity analysis. The DDR's can be assembled directly or obtained on an energy basis.

The well-known equality relating internal strain energy and external work can be written for a discrete structure (n,m) in the following form:

$$\frac{1}{2}\{F\}^T\{\beta\} = \frac{1}{2}\{X\}^T\{P\} \tag{18a}$$

where {X} are the nodal displacements. Equation (18a) can be rewritten by eliminating loads {P} in favor of forces {F} and using the EE ([B]{F} = {P}) to obtain the following relationship:

$$\frac{1}{2}\{X\}^T[B]\{F\} = \frac{1}{2}\{F\}^T\{\beta\} \tag{18b}$$

or

$$\frac{1}{2}\{F\}^T\left([B]^T\{X\} - \{\beta\}\right) = 0 \tag{18c}$$

Since the force vector {F} is not a null set, we finally obtain the following relation between member deformations and nodal displacements:

$$\{\beta\} = [B]^T\{X\} \tag{19}$$

The expression given by equation (19) is the general DDR applicable to finite element models whose EE's can be symbolized as [B] {F} = {P}. In the DDR n deformations are expressed in m displacements; thus there are $r = (n-m)$ constraints on deformations that represent the CC's of the structure (n,m). The CC's are used to augment the EE's, completing them to an $n \times n$ set. The $r = (n-m)$ CC's, which are obtained by eliminating m displacements from n DDR, can be symbolized in matrix notation as

$$[C]\{\beta\} = \{0\} \tag{20}$$

In equation (20), [C] is the $(r \times n)$ compatibility matrix. It is a kinematic relationship and as such it is independent of design parameters, material properties, and external loads. The matrix is rectangular and banded. The maximum bandwidth of CC matrix [C] of an element in a finite element model depends on the force degrees of freedom (fof) of its neighboring elements. The maximum bandwidths of the compatibility conditions for the plate in flexure with fof = 9 shown in figure 2 are as follows: the maximum bandwidths (MBW) of compatibility conditions for the plate can be obtained as a function of the element location in the finite element model as

Interior element MBW = 81	Zone 1
Boundary element MBW = 54	Zone 2
Corner element MBW = 36	Zone 3

The generation of banded compatibility conditions is amenable to computer automation (refs. 11 and 12). The compatibility conditions of finite element analysis are illustrated by taking the example of a stiffened membrane (fig. 3). The finite element model of the structure consists of 9 triangular membrane elements and 23 bars. Each membrane element has three fof; the bar has one fof. The total number of force variables is $n = 50$, consisting of $9 \times 3 = 27$ membrane forces and 23 bar forces. The structure has 11 nodes, each free node has two dof. Node 1 is fully restrained; node 11 is partially restrained. The number of displacement degrees of freedom $m = (11 \times 2 - 2 - 1) = 19$. It has $r = (n-m) = 31$ compatibility conditions. The CC's in terms

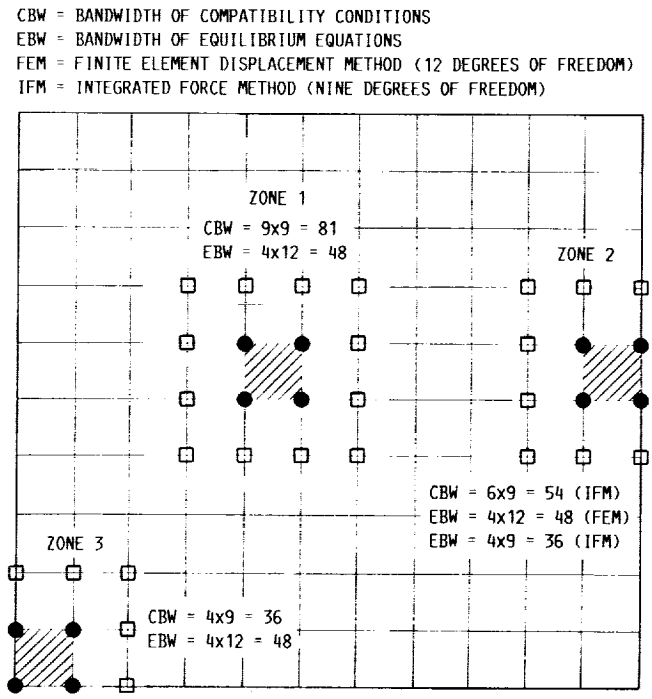

Figure 2.—Bandwidth of compatibility conditions and equilibrium equations for clamped plate.

of member deformations as obtained from St. Venant's strain formulation for finite element analysis of the stiffened membrane are as follows:

$$\beta_4 + \beta_{26} = 0 \tag{21-1}$$

$$\beta_1 + \beta_{24} = 0 \tag{21-2}$$

$$\beta_5 + \beta_{25} = 0 \tag{21-3}$$

$$\beta_2 + \beta_{27} = 0 \tag{21-4}$$

$$\beta_6 + \beta_{28} = 0 \tag{21-5}$$

$$-\beta_{26} + \beta_{29} = 0 \tag{21-6}$$

$$\beta_6 + \beta_{30} = 0 \tag{21-7}$$

$$\beta_{10} + \beta_{31} = 0 \tag{21-8}$$

$$\beta_8 + \beta_{32} = 0 \tag{21-9}$$

$$\beta_7 + \beta_{33} = 0 \tag{21-10}$$

$$\beta_{11} + \beta_{34} = 0 \tag{21-11}$$

$$-\beta_{32} + \beta_{35} = 0 \tag{21-12}$$

$$\beta_{11} + \beta_{36} = 0 \tag{21-13}$$

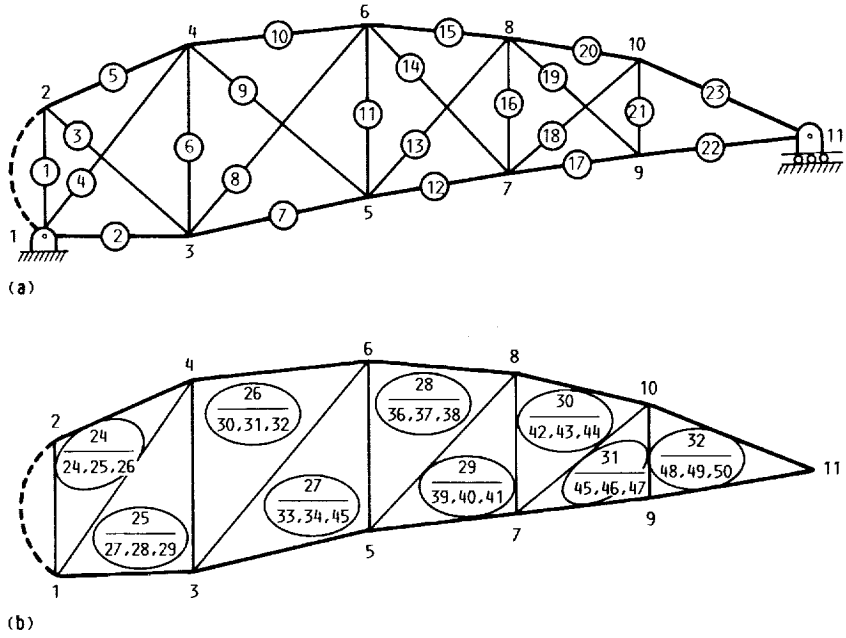

(a) Bar elements.
(b) Membrane elements.

Figure 3.—Idealized stiffened membrane structure.

$$\beta_{15} + \beta_{37} = 0 \qquad (21\text{-}14)$$

$$\beta_{13} + \beta_{38} = 0 \qquad (21\text{-}15)$$

$$\beta_{12} + \beta_{39} = 0 \qquad (21\text{-}16)$$

$$\beta_{16} + \beta_{40} = 0 \qquad (21\text{-}17)$$

$$\beta_{13} + \beta_{41} = 0 \qquad (21\text{-}18)$$

$$\beta_{17} + \beta_{45} = 0 \qquad (21\text{-}19)$$

$$\beta_{16} + \beta_{42} = 0 \qquad (21\text{-}20)$$

$$\beta_{20} + \beta_{43} = 0 \qquad (21\text{-}21)$$

$$\beta_{44} + \beta_{47} = 0 \qquad (21\text{-}22)$$

$$\beta_{21} + \beta_{46} = 0 \qquad (21\text{-}23)$$

$$\beta_{21} + \beta_{48} = 0 \qquad (21\text{-}24)$$

$$\beta_{23} + \beta_{49} = 0 \qquad (21\text{-}25)$$

$$\beta_{18} + \beta_{47} = 0 \qquad (21\text{-}26)$$

$$\beta_{22} + \beta_{50} = 0 \qquad (21\text{-}27)$$

$$-0.1041\beta_1 - 0.7449\beta_2 + \beta_3 - 0.8310\beta_5 - 0.7185\beta_6 - 0.1319\beta_{26} = 0 \qquad (21\text{-}28)$$

$$-0.7223\beta_6 - 0.8049\beta_7 + \beta_9 - 0.7869\beta_{10} - 0.8199\beta_{11} - 0.1205\beta_{32} = 0 \qquad (21\text{-}29)$$

$$-0.7186\beta_{11} - 0.7092\beta_{12} + 0.1104\beta_{13} + \beta_{14} - 0.6954\beta_{15} - 0.8577\beta_{16} = 0 \qquad (21\text{-}30)$$

$$0.5466\beta_{16} - 0.1068\beta_{19} + 0.8018\beta_{20} + 0.8069\beta_{21} - 0.7848\beta_6 + \beta_{47} = 0 \qquad (21\text{-}31)$$

The maximum bandwidths predicted from compatibility conditions and their actual values are shown in table VI. The average number of entries in cc's is much smaller than the predictions from maximum bandwidth considerations. For the example of the stiffened membrane there are 31 cc's; 27 of these cc's have two entries each and the remaining 4 cc's have six nonzero elements. Typically the compatibility matrix is much sparser than most other matrices of structural analysis.

TABLE VI.—BANDWIDTH OF COMPATIBILITY CONDITIONS

Prediction from bandwidth consideration		Actuals		
Maximum	Minimum	Maximum	Average	Minimum
52	18	6	[a]3	2

[a]Rounded to next higher number.

Physical Interpretation of Compatibility Conditions

A finite element model has numerous interelement boundaries. From the viewpoint of continuum analysis the boundary compatibility conditions along these interelement boundaries also have to be satisfied. The conditions along the element interface can be symbolized as

$$\delta_{RI} + \delta_{RII} = 0 \tag{22a}$$

where (δ_{RI},δ_{RII}) represent the residue in the BCC's of the two neighboring elements I and II, respectively. For the membrane problem the residue δ_R can be represented in the following form (ref. 7):

$$\delta_R = \left(\frac{1}{E}\right)\left[\frac{\partial}{\partial x}(N_y - \nu N_x)n_x + \frac{\partial}{\partial x}(N_x - \nu N_y)n_y - (1+\nu)\left\{\frac{\partial}{\partial x}(N_{xy})n_y + \frac{\partial}{\partial x}(N_{xy})n_x\right\}\right] \tag{22b}$$

where N_x, N_y, and N_{xy} are the membrane stress resultants and n_x and n_y represent the direction cosines of the outward normal for the element interface.

The equality constraint given by equation (22a) ensures interelement boundary compatibility. The correct stress fields should satisfy the interelement BCC's given by equation (22a). Element interphase boundaries could be of complicated geometry; in consequence it is rather difficult to explicitly satisfy the interelement BBC's given by equation (22a) apriori by choosing appropriate displacement or stress fields, or both. The satisfaction of interelement strain compatibility, and not just displacement continuity, is a neglected condition in the popular stiffness method formulation. In general, stresses obtained by displacement formulation along the element interface boundary satisfy neither equilibrium nor compatibility conditions. (Because of this limitation in the stiffness-based finite element method, stress computation is typically avoided at the cardinal node points or along element interphases.)

In the integrated force method interelement BBC's are automatically enforced via the CC's

$$[C]\ \{\beta\} = [C]\ [G]\ \{F\} = \{\delta R\}$$

Take the example of the stiffened membrane shown in figure 3. The CC's between elements at interfaces are satisfied by the constraints given by equations (21-1) to (21-27). Take equation (21-12) for example. This constraint enforces interelement deformation continuity or BCC's between membrane elements 26 and 27 along the interelement boundary defined by nodes 3 to 6 as depicted in figure 4(a). Such interelement CC's are designated by the symbol (MM), membrane-to-membrane compatibility, in figure 4(a). Take the next CC given by equation (21-13). This constraint enforces deformation balance conditions between membrane 27 and bar 11 along the interface defined by nodes 5 and 6. These types of CC's are symbolized by BM, bar-to-membrane compatibility, in figure 4(a). The total number of interphase CC's (both MM and BM) is 27 as shown in figure 4(a). Besides these CC's there are four bay CC's; these enforce deformation balance conditions of six adjoining bars as shown in figure 4(b).

In the integrated force method the equilibrium conditions are satisfied at the nodes [B] {F} = {P}, the same as attempted by the stiffness method. In addition, the following CC's are satisfied only in the IFM:

(1) Membrane-to-membrane compatibility

(2) Membrane-to-bar compatibility

(3) Compatibility between a group of bars

For this example the EE's number 19 and the CC's number 31. The IFM satisfies all 50 equations. In contrast, the stiffness method is based on the 19 EE's expressed in displacements; the 31 CC's are more or less ignored. Since it is mandatory for the stress fields to satisfy the CC's, their exclusion in the stiffness method reflects on the accuracy of the stress fields.

Computer Automation of Formulations

Modern structures, because of their complexity, have to be analyzed by digital computers. Computer automation is therefore an essential requirement of analysis formulation despite its other merits and limitations. The integrated force method satisfies this requirement, since all three matrices (equilibrium matrix [B], compatibility matrix [C], and flexibility matrix [G]) are amenable to automatic generation on a digital computer. Since the stiffness method is known to be amenable to computer automation, both the IFM and the SM satisfy this requirement.

Solution Accuracy

The accuracy of solutions obtained either by IFM or SM is of paramount importance in the choice of analysis formulation. During the formative period of finite element analysis Argyris (refs. 21 and 22) solved several problems both by the classical force method (SFM) and the stiffness method. Scrutiny of this

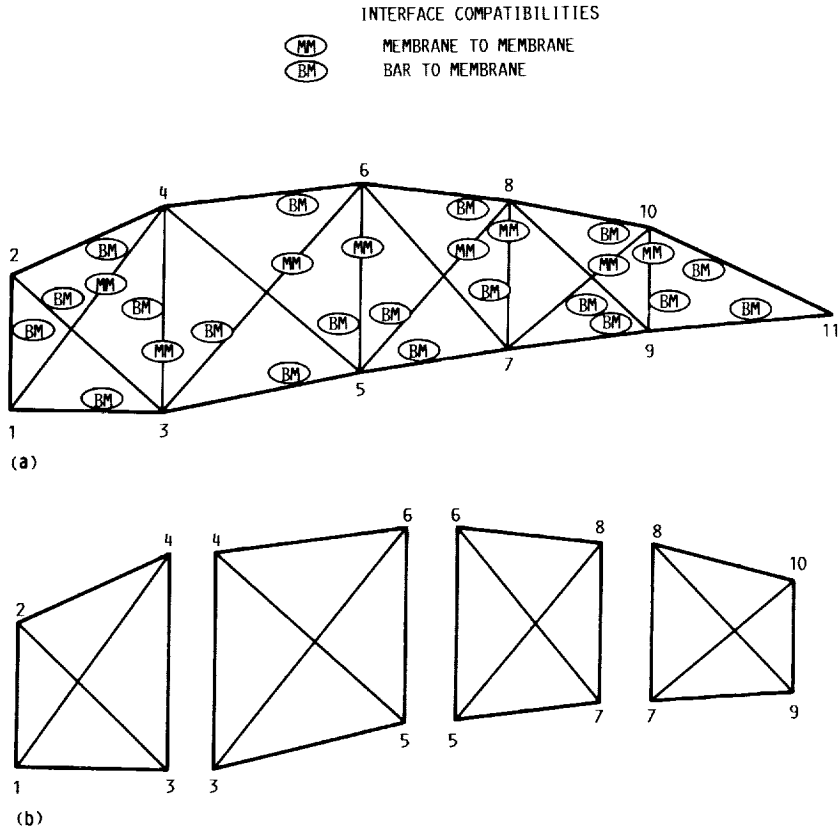

(a) Interface.
(b) Bay.

Figure 4.—Compatibilities of stiffened membrane structure.

study indicates that the SFM predicted more accurate stress solutions for almost all examples, including plates and cylinders, whereas inaccuracies can be noticed in the stiffness computations. The IFM retains all the favorable features of the classical force method (SFM) as far as solution accuracy is concerned. Consequently IFM predictions have to be as accurate as Argyris's SFM results.

To check the accuracy of solutions between the integrated force method and the stiffness method in the context of finite element analysis, we developed two plate bending elements for the IFM:

(1) A rectangular element with four nodes

(2) A triangular element with three nodes

The quality of solutions obtained by the IFM and the SM was compared for both types of elements by taking the example of clamped plate bending under a concentrated load. The plate parameters were as follows:

Size of plate, $a = b$, in. (cm) 40 (101.6)
Thickness of plate, h, in. (mm) 0.2 (5.08)
Young's modulus, E, ksi (kg/mm^2).... 30 000 (21 091.81)
Poisson's ratio, ν..... 0.3
Magnitude of concentrated load at
center, P, lb (kg) 500 (226.795)

In the stiffness method nodal stress parameters calculated by backsubstituting from grid point displacements are discontinuous and ambiguous (ref. 9). Calculating forces at the nodes is routinely avoided in the stiffness method. Because of that the noncontroversial nodal displacement was used in the comparison. It should, however, be remembered that in the IFM forces are the primary variables from which displacements are obtained by backsubstitution.

The central deflection of the plate given by Timoshenko (ref. 20) is

$$w_c = 0.2036 \text{ in. } (5.715 \text{ mm})$$

For the stiffness analysis two well-known analysis codes, ASKA (ref. 23) and MSC/NASTRAN (ref. 24), were used. The types of plate bending elements used were

(1) QUAD-4: Rectangular element with 12 degrees of freedom. Both ASKA and MSC/NASTRAN have QUAD-4 elements.

(2) TRIB-3: Triangular element of the ASKA program with nine degrees of freedom.

(3) TUBA-3: Higher order triangular element of the ASKA program with 18 degrees of freedom.

(4) TRIA-3: Triangular element of MSC/NASTRAN with nine degrees of freedom.

The first three elements are well known in the literature and are popular in practice. The QUAD-4, a quadrilateral element with six dof per node was used here as a rectangular flat-plate element with three dof at grid points with appropriate specialization. Likewise flat-plate elements were obtained from the triangular elements of the general-purpose program.

Analysis by ASKA Code

QUAD-4 is a rectangular element, it has three dof per node, consisting of transverse displacement w and two rotations (θ_x and θ_y), and its in-plane rotation is restrained. The element displacement field corresponds to a cubic displacement function with 12 constants. TRIB-3 and TUBA-3 of the ASKA code are triangular elements. TUBA-3 is a higher order element with 18 degrees of freedom. It has six degrees of freedom per node consisting of one displacement, two slopes, and three curvatures. TRIB-3 is a plate element with 9 degrees of freedom. It has three degrees of freedom per node consisting of one displacement w and two rotations (θ_x and θ_y).

The results obtained for the central displacement w_c by using ASKA QUAD-4, TRIB-3, and TUBA-3 elements are presented in table VII for several finite element idealizations, shown in figure 5. The central displacement obtained by using the ASKA QUAD-4 element tended to converge to Timoshenko's solution for the finite element model with 64 and 100 elements at a residual error of about 2 percent. As table VII shows, there was no substantial difference in the convergence rate for the two triangular elements. As before, the stiffness method required a very fine mesh of about 128 elements to show some convergency to the closed-form solution. For the 128-element model the residual error was about 10 percent for TUBA-3 and 6 percent for TRIB-3.

MSC/NASTRAN Verification

The example of a clamped plate under a central concentrated load as shown in figure 1 was again solved, this time by using

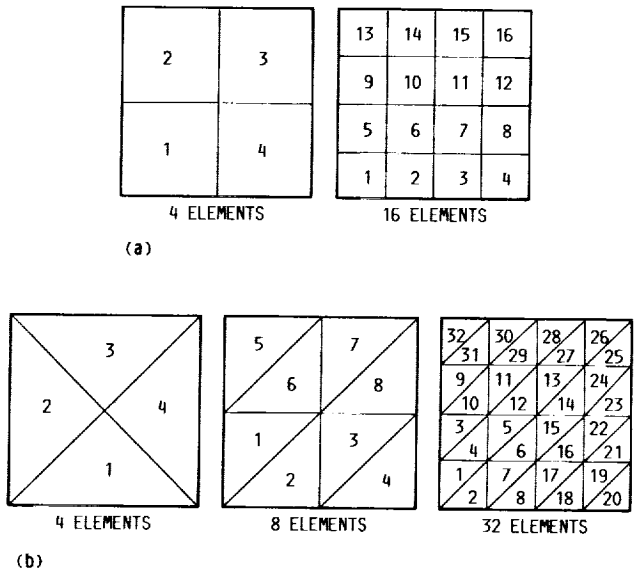

(a) Rectangular elements.
(b) Triangular elements.

Figure 5.—Discretization of plate by using rectangular and triangular finite elements.

the QUAD-4 element of the NASA structural analysis code MSC/NASTRAN. The QUAD-4 elements of the MSC/NASTRAN and ASKA codes are identical with respect to the two fundamental element characteristics, such as the number of nodes and the grid point displacement degrees of freedom. Results obtained for three models with 4, 16, and 36 elements, respectively, are presented in table VIII.

As tables VII and VIII show, the agreement in the results obtained by the two codes (MSC/NASTRAN and ASKA) for the problem was good. For 4 and 16 elements the ASKA results were marginally better than the MSC/NASTRAN solution. However, MSC/NASTRAN showed monotonic convergence with a residual error of 0.29 percent for the 36-element model,

TABLE VII.—ASKA CODE ANALYSIS RESULTS

[Timoshenko's solution, w_c = 0.2036 in. (5.715 mm).]

Number of elements	QUAD-4 rectangular element			TRIB-3 triangular element			TUBA-3 triangular element		
	Central displacement, w_c		Error, percent	Central displacement, w_c		Error, percent	Central displacement, w_c		Error, percent
	in.	mm		in.	mm		in.	mm	
4	0.0409	1.0388	80.00	0.0860	2.1844	57.76	0.0771	1.9583	62.13
8	———	———	———	.0650	1.6510	68.07	.0641	1.628	68.51
16	.1995	5.0673	2.04	———	———	———	———	———	———
32	———	———	———	.1547	3.9294	24.01	.1607	4.0818	21.07
64	.2092	5.3137	2.75	———	———	———	———	———	———
100	.2092	5.3137	———	———	———	———	———	———	———
128	———	———	2.75	.1837	4.6660	9.82	.1910	4.8514	6.18

TABLE VIII.—MSC/NASTRAN AND IFM ANALYSIS RESULTS

[Timoshenko's solution, w_c = 0.2036 in. (5.1715 mm).]

Number of elements	NASTRAN QUAD-4			IFM rectangular element		
	Central displacement, w_c		Error, percent	Central displacement, w_c		Error, percent
	in.	mm		in.	mm	
4	0.027	0.686	86.75	0.2041	5.1842	0.20
16	.1914	4.862	6.02	.2035	5.1689	.05
36	.2042	5.187	.29	.2035	5.1689	.05

whereas the ASKA code exhibited a residual error of about 2 percent for a 100-element model.

Analysis by Integrated Force Method

The IFM rectangular element assumes cubic distribution for displacements (eq. (11) or (13)) and linear distribution for forces (eq. (10)). This element corresponds to the QUAD-4 element, which also has three displacement degrees of freedom per node, consisting of displacement w and two slopes (θ_x and θ_y) for its four nodes. As far as displacement and force degrees of freedom and number of nodes are concerned, all three elements (IFM, ASKA, and MSC/NASTRAN) are equivalent. The results obtained by IFM for three different finite element models are given in table VIII. Remember that in IFM the forces are calculated first and then the desired displacements are obtained from the forces by backsubstitution. For the purpose of comparison, however, only displacement is presented, since only this variable is directly calculated in the stiffness method as mentioned before.

Table VIII shows that convergence occurred for the first model, consisting of four elements. If symmetry is taken into consideration, convergence will occur for a single element. The residual error for the four-element model was 0.2 percent, and it was reduced to 0.05 percent for the second model, which had 16 elements. Results obtained for the rectangular element by using IFM and the two well-known displacement-based finite element programs (ASKA and MSC/NASTRAN) are presented graphically in figure 6. The IFM results are barely discernible from Timoshenko's solution, whereas the ASKA and MSC/NASTRAN results converge slowly.

MacNeal and Harder (ref. 25) introduced a grading scheme for the evaluation of finite elements, as follows:

A = less than 2 percent error
B = 2 to 10 percent error
C = 10 to 20 percent error
D = 20 to 50 percent error
F = greater than 50 percent error

The comparative merits of IFM, ASKA, and MSC/NASTRAN results on the basis of residual error are given in table IX, which is based on MacNeal's grading scheme. The IFM element

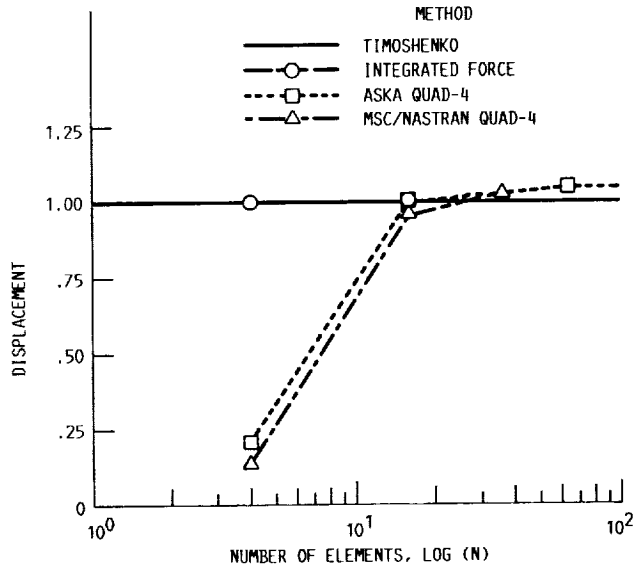

Figure 6.—Convergence analysis of clamped plate with concentrated load by using rectangular or quadrilateral finite elements.

scored an "A" grade for the first model, consisting of four elements only. MSC/NASTRAN QUAD-4 required 36 elements to reach "A", and ASKA QUAD-4 was unable to achieve an "A" even with 100 elements.

Results for Triangular Elements

The convergency for the problem using triangular elements of the IFM and stiffness codes (ASKA and MSC/NASTRAN) is presented in figure 7. The grades secured by the elements are given in table IX. The IFM result was discernible from the

TABLE IX.—MacNEAL'S GRADE CARD

(a) Rectangular element "report card"

Number of elements	IFM rectangular	MSC/NASTRAN QUAD-4	ASKA QUAD-4
4	A	F	F
16	A	B	B
36	A	A	B
64	—	A	B
100	—	—	—

(b) Triangular element "report card"

Number of elements	IFM rectangular	MSC/NASTRAN TRIA-3	ASKA	
			TRIB-3	TUBA-3
4	B	F	—	F
8	A	D	F	F
16	—	C	—	—
32	—	B	C	D
128	—	—	B	B

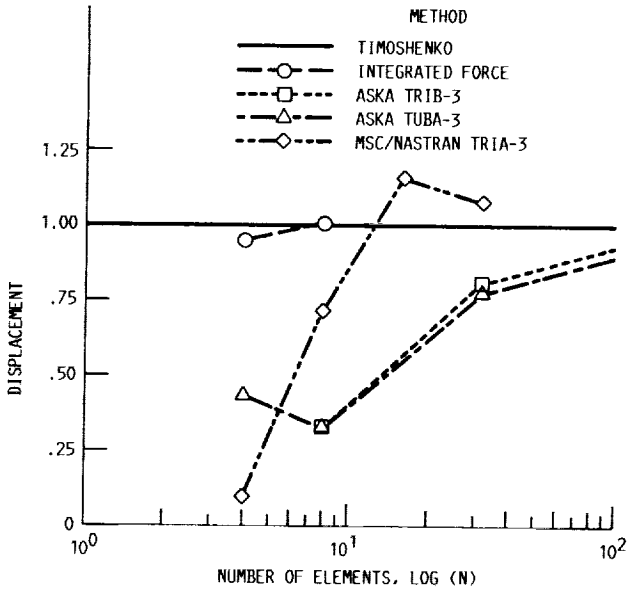

Figure 7.—Convergence analysis of clamped plate with concentrated load by using triangular finite elements.

analytical solution for the first model, with four elements, but even so it displayed engineering accuracy. The next model, with eight elements, converged to the analytical solution and also achieved grade "A."

Displacement-based triangular plate bending elements are known to be overly stiff and exhibit slow convergence, as can be seen from figure 7. Neither MSC/NASTRAN nor ASKA elements could achieve grade "A." The MSC/NASTRAN and ASKA analyses required 32 and 128 elements, respectively, to reach a "B" grade.

From solutions presented in this report and from Argyris's examples it is clear that the IFM yields results that are superior to those obtained by the stiffness method. The reason is that the IFM satisfies both the EE's and the CC's explicitly and simultaneously (eq. (1)) whereas the stiffness method attempts to satisfy equilibrium equations via displacements (eq. (3)). In approximate methods (such as IFM and SM) one cannot expect accurate response prediction when some analysis equations are neglected, as is the case with the stiffness method.

Element Level Effect

To examine the effect of different types of elements on overall response accuracy, we obtained the central deflection of the clamped plate by using the following rectangular element types.

(1) Stiffness-based plate bending elements
  (a) ASKA QUAD-4 element
  (b) MSC/NASTRAN QUAD-4 element

(2) IFM-based plate bending elements
  (a) Przemieniecki's element
  (b) IFM consistent element I (displacement field defined by eq. (11))
  (c) IFM consistent element II (displacement field defined by eq. (13))

The elements are equivalent with respect to displacement and force field assumptions, being cubic and linear, respectively, which gives rise to 12 degrees of freedom at the four nodes of the element. The elements differ with respect to assumed polynomials, such as defined by equations (11) and (13) for the IFM. The results obtained for the five types of elements are presented in table X. As table X shows

(1) In the stiffness method the nature of the polynomials used influenced the overall response to a limited extent such as 86 percent versus 80 percent, 6 percent versus 2 percent, etc., between MSC/NASTRAN and ASKA elements.

(2) In the IFM the nature of the polynomials (eqs. (11) and (13)) had a negligible effect on the results as can be seen for IFM elements I and II.

(3) Przemieniecki's element, which was obtained by direct application of the law of equilibrium, can be backcalculated to correspond to a rather poor displacement distribution. This least-sophisticated element, developed three decades ago, still yielded acceptable response for the difficult test problem. The point here is that the driver for overall solution accuracy in the IFM is satisfaction of the system equilibrium and global cc's; the element quality or the type of interpolation polynomial used play a rather less significant role.

TABLE X.—ELEMENT LEVEL EFFECT

Number of elements	Stiffness method		Integrated force method		
	MSC/NASTRAN	ASKA	Consistent $[B]_s$	Consistent $[B]_a$	Lumped $[B]_P$ (Przemieniecki)
	QUAD-4		Rectangular element		
	Error in central displacement, percent				
4	86.75	80.00	0.20	0.20	24.11
16	6.02	2.04	.05	.05	35.29
36	.29	———	.05	.05	———
64	———	2.75	———	———	———
100	———	2.75	———	———	———

Conditioning of Equations of IFM Versus SM

Finite element analysis requires the solution of a large number of simultaneous equations. Hence the stability of the equation is a primary criterion in the choice of analysis formulation. The IFM matrix [S] is not symmetric, whereas the SM stiffness matrix [K] is symmetric. The matrix [S] is of higher dimension than the stiffness matrix [K]. The norms of the IFM upper equilibrium matrix [B] and lower CC matrix [G] in equation (1) differ substantially. It may therefore be suspected that the IFM equation that contains both EE's and CC's is an ill-conditioned system. In order to examine the issue, we analyzed several problems (1) by scaling the CC's and (2) without any scaling at all. Scaling had no effect on the solution: the IFM lost only one or two precision points in 14-digit arithmetic for almost all problems solved.

We further compared IFM and SM equations numerically for a few different types of structures. The equation stability of SM is governed by the parameter z, defined as

$$z = \frac{\lambda_{max}}{\lambda_{min}} \tag{23a}$$

where λ_{max} and λ_{min} are the maximum and minimum eigenvalues, respectively, of the symmetric stiffness matrix [K]. The equation stability of IFM matrix [S] is governed by the parameter y defined as

$$y = \frac{S_{max}}{S_{min}} \tag{23b}$$

where S_{max} and S_{min} are the maximum and minimum singular values, respectively, of the nonsymmetric matrix [S]. We evaluated z and y for several structure types and some results are presented in table XI. For the examples solved, the eigenspace of matrix [S] was much less distorted than that of the stiffness matrix [K]; that is,

$$e = \frac{z}{y} >> 1 \quad \text{or} \quad z >> y \tag{24}$$

Since z is greater than y, the IFM equations were more stable than the SM equations. One need not be influenced by the simple fact that the SM stiffness matrix [K], being symmetric, should possess better conditioning than the IFM matrix [S]. The reason is that the symmetric stiffness matrix [K] is a product of three matrices, $[K] = [B]\ [G]^{-1}[B]^T$, and successive matrix multiplications and inversions deteriorate its stability. The IFM matrix [S] is well conditioned. The integrated force method thus gave rise to a superior set of equations than did the stiffness method.

TABLE XI.—STABILITY OF EQUATIONS—STIFFNESS METHOD VERSUS INTEGRATED FORCE METHOD

Type of structure	Stiffness method, $z = \lambda_{max}/\lambda_{min}$	Integrated force method, $y = S_{max}/S_{min}$
Truss (6,4)	16.47	2.96
Truss (16,13)	218.50	3.17
Truss (26,21)	1 598.10	7.31
Truss (36,29)	3 378.37	45.89
Frame (9,6)	1 335.96	3.65
Frame (18,12)	7 840.99	6.96
Frame (27,18)	21 573.55	10.20
Frame (36,24)	34 533.71	7.48
Plate (9,6)	4 790.65	18.75
Plate (18,12)	23 759.55	29.89
Plate (27,18)	51 089.50	56.11
Plate (36,24)	75 191.74	64.56

Sparsities of [B], [C], [S], and [K] Matrices

Comparison of Sparsities

Matrix sparsity and bandwidth are important parameters in the finite element analysis. These parameters of the compatibility matrix [C] were compared with the same parameters of the equilibrium matrix [B] for three types of structures designated according to the notation introduced earlier as truss (101,81), frame (99,66), and plate (99,66). The structures are shown in figure 8. The properties of the associated symmetric stiffness matrix [K] were included for baseline reference. The parameters of the matrices are tabulated in table XII. As can be seen, the sparsities of the EE matrix [B] and the CC matrix [C] were comparable but smaller than those of the stiffness matrix [K]. The bandwidths of the matrices [B], [C], and [K] were more or less comparable. Within the bands the matrices [B] and [C] were sparser than the stiffness matrix [K]. The flexibility matrix [G] is a concatenated matrix, and its maximum bandwidth, which depends on the number of force variables of the elements, was much smaller than dimension n of matrix [S]. The internal sparsity of the flexibility matrix enhanced the zero population of the system matrix. The sparsities of the matrices [S], [C], and [B] for three other structures are shown in table XII.

From table XII and several other examples solved, it was a common observation that the governing IFM matrix [S] was much sparser than the equilibrium matrix [B] or the stiffness matrix [K]. As already noted, the compatibility matrix [C] appeared to be the sparsest among the structural analysis matrices ([B], [S], and [K]).

Sparsity Growth During Factorization of Matrix [S]

The IFM equation system has population along two diagonals as depicted in figure 9(a): EE population along the top diagonal

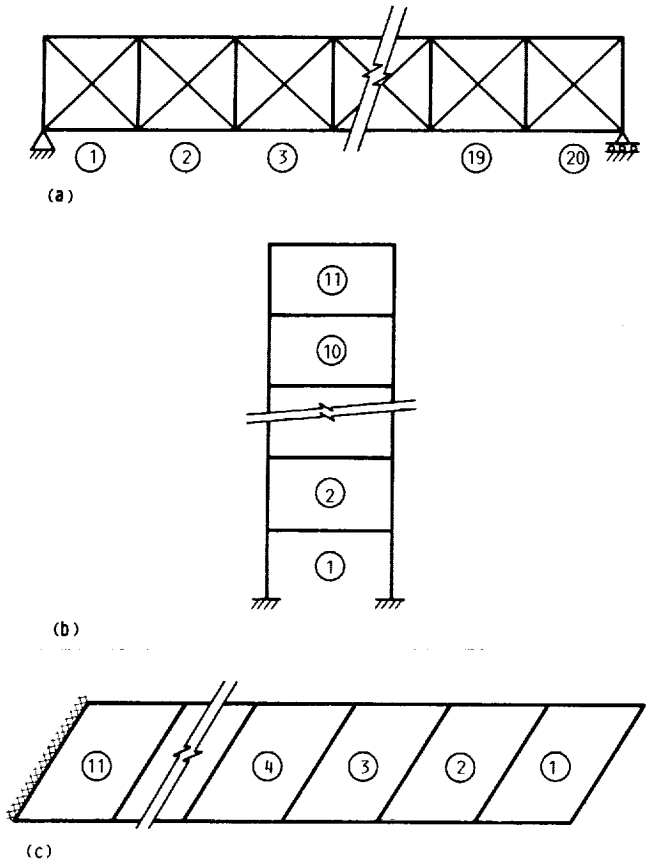

(a) Twenty-bay truss.
(b) Eleven-story frame.
(c) Eleven-element cantilevered plate.

Figure 8.—Three structures used.

and CC population along the bottom diagonal. This unconventional feature of the [S] matrix was avoided by generating adequate numbers of EE's followed by CC's based on CC bandwidth information. The process was repeated and a banded [S] matrix was obtained as depicted in figure 9(b). Sparse matrix algebra along with a nonsymmetric matrix solver (LA05 (ref. 26)) is used for IFM analyses. In order to avoid the deterioration of sparsity during solution, the symmetric stiffness matrix is typically factored ([K] = [L] [U]), where the [L] and [U] are upper and lower triangular matrices. The population inside the band for the symmetric stiffness matrix [K] is equal to the sum of its factors ([L] + [U]). The question is, What is the sparsity increase during the factoring of the [S] matrix? This issue ([S] = [L][U]) was examined numerically for a few examples, as given in table XIII. The factoring was carried out by the Harwell library sparse solver LA05. In the examples solved, the actual nonzero population of the sum of the triangular matrices ([L] + [U]) was somewhat less than the sparsity of the [S] matrix. The program LA05, however, printed a minor growth in sparsity ratio. This deviation was not a deficiency of the structure of the [S] matrix but was attributed to the storage scheme used and to the degree of compaction in the algorithm at the time of printing.

Comparison of Computation Time

The IFM matrix [S] is unsymmetrical and its dimension is $(n \times n)$. The SM matrix [K] is symmetrical and its dimension is $(m \times m)$, where $n \geq m$. From this information alone, for identical idealization of a structure with the same number of elements it can be argued that solution by IFM should be numerically more expensive than solution by SM. To examine this issue, we solved three examples (a truss, a frame, and a plate, each with approximately 100 degrees of freedom) for

TABLE XII.—SPARSITY OF MATRICES [B], [C], AND [K]

Type of structure	Matrix								
	[B]	[C]	[K]	[B]	[C]	[K]	[B]	[C]	[K]
	Sparsity, percent			Bandwidth					
				Average			Maximum		
Truss (101,81)	4.82	5.94	14.5	8	6	10.91	8	6	12
Frame (99,66)	6.85	6.52	17.34	11.45	12.45	10.91	12	14	12
Plate (99,66)	4.53	4.44	25.91	17.18	8.82	17.10	18	16	18

Type of structure	Sparsity ratio		
	[S]	[B]	[C]
Truss (176,141)	0.022	0.020	0.034
Plate (144,27)	.075	.126	.039
Plate (36,3)	.144	.450	.036

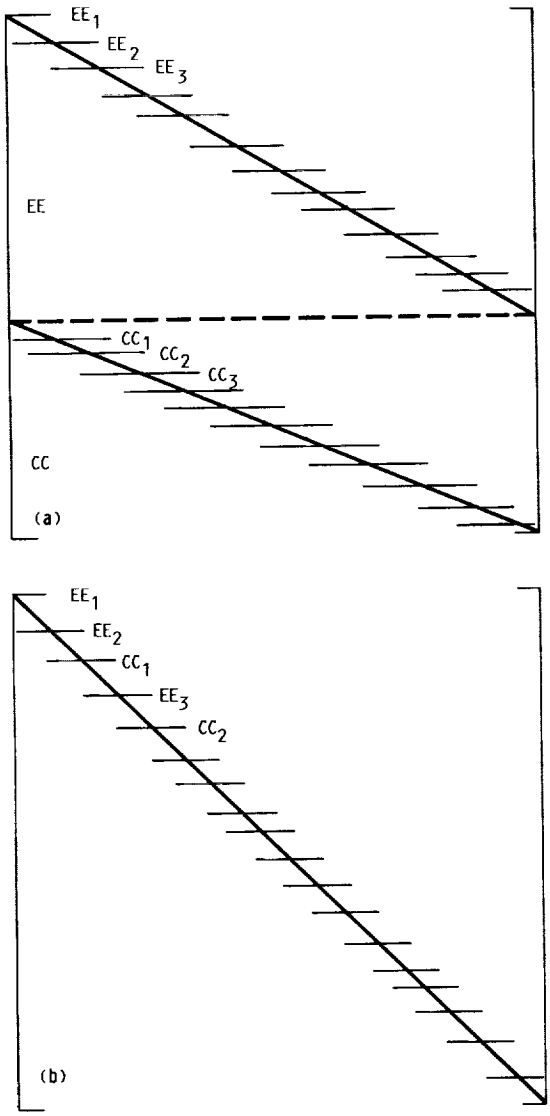

(a) EE and CC matrices separated.
(b) EE and CC matrices intermingled.

Figure 9.—Population distribution in matrix [S].

forces and displacements by the IFM, SM, and SFM methods on the same computer hardware and with the same software techniques. The number of elements and the finite element model remained the same for all three analytical methods. The discrete element model utilized the standard flexibility and stiffness matrices for bar and beam elements. For the plate a rectangular element with three degrees of freedom per node was used. These were two moments and a shear force in IFM and two rotations and one transverse displacement in SM. Computation times recorded for the three examples are given in table XIV. Table XIV also shows the solution time by SFM (refs. 1, 4, and 27 to 33) based on the "turn back LU" procedure of Tapsu (ref. 29) and on the LP (linear programming) code (ref. 12). For these examples the IFM required less computation time than the SM. This can be attributed to the following factors:

TABLE XIII.—SPARSITY GROWTH IN LOWER AND UPPER TRIANGULAR FACTORS OF MATRIX [S]

Structure	Matrix [S]	Triangular factors		Sparcity ratio, ([L] + [U])/[S], P/A[a]
		Lower, [L]	Upper, [U]	
	Number of nonzeros in matrices, P/A[a]			
Robinson's rectangular-plate bending element				
Plate (36,3)	280/230	126/15	299/152	1.045/0.661
Plate (144,27)	2056/1553	1263/160	1290/1063	1.202/0.789
IFM consistent element				
Plate (36,3)	300/260	140/10	166/130	1.02/0.538
Plate (144,27)	2212/1852	1359/78	1248/1104	1.179/0.638

[a]P = number of nonzeros as printed out by Harwell subroutine LA05;
A = actual number of nonzeros as counted.

TABLE XIV.—COMPUTATION TIME—INTEGRATED FORCE METHOD VERSUS STIFFNESS METHOD AND STANDARD FORCE METHOD

Type of structure	Integrated force method	Stiffness method	Standard force method	
			LU[a]	LP[b]
	Central processing unit time, sec			
Truss (101,81)	0.72	2.5	2.14	3.14
Frame (99,66)	1.52	2.59	2.28	2.09
Plate (99,66)	1.26	3.1	4.06	3.27

[a]LU: turn back LU (lower and upper triangular factors of a matrix) procedure (ref. 28).
[b]LP: linear programming (ref. 11).

(1) The SM requires a series of transformations and backsubstitutions (from local to global system to generate displacements and then from global to local system to calculate forces). In the IFM most of the transformations are not required.

(2) The IFM element matrices [B] and [G] can be generated in closed form.

(3) For continuum analysis, operations equivalent to differentiation are required to obtain stresses in the SM that are avoided in the IFM.

(4) Equilibrium equations represent a very sparse system of equations in the IFM; but for only $r = (n-m)$ forces, EE's essentially represent a triangular system. As such a comparison of m SM equations to n IFM equations is not truly accurate, one should compare $r = (n-m)$ of IFM to m of SM. This is the traditional comparison between the classical force method (SFM) and SM, and it holds true for IFM in a slightly different scale (refer to appendix A). Thus for a truss (101,81) the IFM solution time should be more or less proportional to $r = 20$ and the SM solution time to 81. As the steps (1) to (4) are less favorable for the stiffness method, the total computation required was less for the IFM than for the SM. In the SFM the

time requirement was on the higher side because generation of a self-stress matrix and redundant segregation involve considerable computation (ref. 12).

Buckling and Dynamic Response Analyses

Stability and vibration response analyses are routinely required in industry. The standard force method cannot be formulated to handle such response analyses directly because in the SFM redundants are treated separately as loads instead of as part of the original structure (ref. 1). The IFM has no such limitations and it has been extended for eigenresponse analysis of both discrete systems and of continua (refs. 1, 10, and 13). To complete the comparison and illustration of the IFM versus the SM, we give the stability and vibration response analyses of the simple three-bar truss shown in figure 10. For these response analyses "force mode shape" was taken as the primary unknown. The inertia and damping parameters were thus written in terms of forces as
Inertia force:

$$[M]\{\ddot{X}\} = [M][J][G]\{\ddot{F}\} \tag{25}$$

Damping force:

$$[D]\{\dot{X}\} = [D][J][G]\{\dot{F}\} \tag{26}$$

where [M] and [D] are the mass and damping matrices, respectively.

With the typical assumption that forces and displacements are harmonic in time, we can write

$$\{F\} = \{F\}_m e^{i\omega t} \tag{27}$$

$$\{X\} = \{X\}_m e^{i\omega t} \tag{28}$$

where ω is radian frequency, $\{F\}_m$ and $\{X\}_m$ are the force and displacement mode shapes, respectively, and i is the imaginary unit.

The IFM dynamic equation can be symbolized as

$$[S]\{F\}_m - i\omega\left[\frac{[D][J][G]}{[0]}\right]\{F\}_m - \omega^2\left[\frac{[M][J][G]}{[0]}\right]\{F\}_m \tag{29a}$$

or

$$[S]\{F\}_m + i\omega[D]_f\{F\}_m + \omega^2[M]_f\{F\}_m = [0] \tag{29b}$$

Here, $[D]_f$ and $[M]_f$ are the damping and mass matrices, respectively, of the IFM.

Frequency analysis by the IFM is illustrated here for a three-bar truss with a mass m_0 as depicted in figure 10. Damping

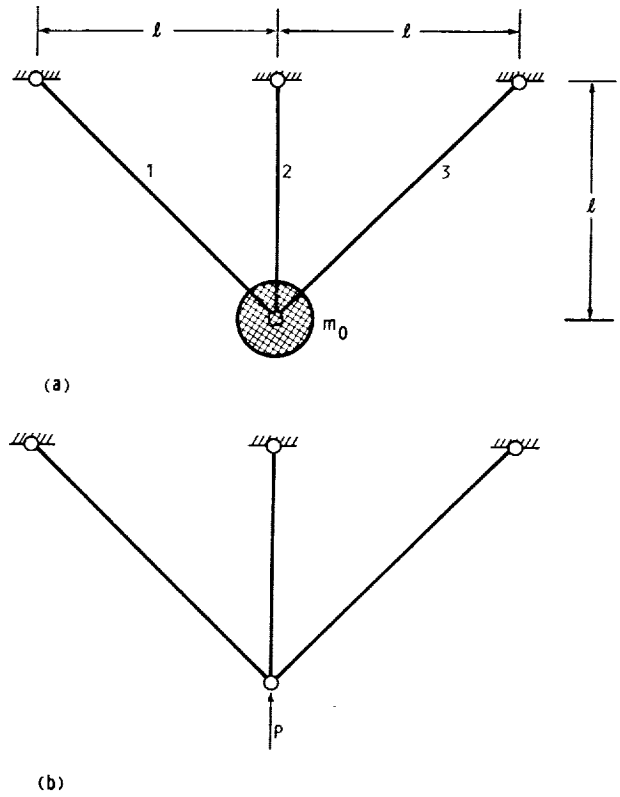

(a) Frequency analysis.
(b) Stability analysis.

Figure 10.—Response analysis of three-bar truss.

and mass of bars were neglected. The matrices $[D]_f$, [S], and $[M]_f$ for a truss are as follows:

$$[D]_f = 0 \tag{30}$$

$$[S] = \begin{bmatrix} \frac{-1}{\sqrt{2}} & 0 & \frac{1}{\sqrt{2}} \\ \frac{1}{\sqrt{2}} & 1 & \frac{1}{\sqrt{2}} \\ \frac{1}{A_1} & \frac{-1}{A_2} & \frac{1}{A_3} \end{bmatrix} \tag{31}$$

$$[M]_f = \frac{m_0}{A_e E}\begin{bmatrix} \sqrt{2}L(A_3 + \sqrt{2}A_2) & L(A_3 - A_1) & -\sqrt{2}(A_1 + \sqrt{2}A_2) \\ -\sqrt{2}LA_3 & -L(A_3 + A_1) & -\sqrt{2}L(A_1) \\ 0.0 & 0.0 & 0.0 \end{bmatrix} \tag{32}$$

where $A_e = (A_1A_2 + A_2A_3 + \sqrt{2}A_1A_3)$ and A_1, A_2, and A_3 are the areas of members 1, 2, and 3, respectively. For $m_0 = 0.68$ slug (1 kgm); A_1, A_2, and $A_3 = 1.0$, 1.0, and 2.0 in.^{2} (645.163, 645.163, and 1290.326 mm^2); and E = 30 000 ksi (21 091.81 kg/mm^2) the frequencies of the structure obtained by solving equation (29a) were

$$f_1 = 102.93 \text{ Hz} \quad \text{and} \quad f_2 = 155.89 \text{ Hz} \tag{33}$$

The mode shapes $\{F\}_1$ and $\{F\}_2$ for frequencies f_1 and f_2, respectively, were

$$\{F\}_1 = \begin{Bmatrix} -0.996 \\ -0.466 \\ 1.000 \end{Bmatrix} \tag{34}$$

$$\{F\}_2 = \begin{Bmatrix} 0.259 \\ 0.759 \\ 1.000 \end{Bmatrix} \tag{35}$$

Displacement modes were obtained from force modes by backsubstituting in equation (2). The displacement modes were

$$\{X\}_1 = \begin{Bmatrix} 1.000 \\ -0.318 \end{Bmatrix} \tag{36}$$

$$\{X\}_2 = \begin{Bmatrix} 0.318 \\ 1.000 \end{Bmatrix} \tag{37}$$

Vibration analysis of the structure by using the ASKA code was also performed, and identical results were obtained. Solutions of eigenvalue and dynamic excitation problems are reported in references 10 and 13.

Stability Analysis

The IFM has been extended to stability analysis of structures (ref. 1). The stability analysis equations were obtained by following the usual perturbation theory. The key equation for stability analysis by the IFM is

$$[S]\{F\} = \lambda[K]_g[J][G]\{F\} \tag{38a}$$

or

$$[[S] - \lambda[S]_b]\{F\} = \{0\} \tag{38b}$$

where $[K]_g$ is the geometric stiffness matrix and λ is the stability parameter. The matrix $[S]_b$ is referred to as "the IFM stability matrix."

The stability analysis was illustrated once again by using the example of a three-bar truss. The stability equation for the three-bar truss (refs. 2 and 3) for equal bar areas of 1 in.^{2} (645.163 mm^2) has the following form:

$$\begin{bmatrix} 0.707 + 0.793\left(\frac{\lambda}{E}\right) & 0 & 0.707 - 0.793\left(\frac{\lambda}{E}\right) \\ -0.707 - 0.086\left(\frac{\lambda}{E}\right) & 0.121\left(\frac{\lambda}{E}\right) & -0.707 - 0.085\left(\frac{\lambda}{E}\right) \\ 1 & -1 & 1 \end{bmatrix} \begin{bmatrix} \{F\}_1 \\ \{F\}_2 \\ \{F\}_3 \end{bmatrix} = 0 \tag{39}$$

Solution of the stability equation yielded the following results:

(1) Buckling loads

$$P_{1,crt} = 0.891E, \quad P_{2,crt} = 8.248E \tag{40}$$

(2) Force mode shapes

$$\{F\}_1 = \begin{Bmatrix} 1.000 \\ 0.000 \\ -1.000 \end{Bmatrix} \tag{41}$$

$$\{F\}_2 = \begin{Bmatrix} 0.500 \\ -1.000 \\ 0.500 \end{Bmatrix} \tag{42}$$

(3) Displacement mode shapes

$$\{X\}_1 = \begin{Bmatrix} -1.000 \\ 0.000 \end{Bmatrix} \tag{43}$$

$$\{X\}_2 = \begin{Bmatrix} 0.000 \\ 1.000 \end{Bmatrix} \tag{44}$$

The stability problem was also solved with the ASKA code and identical solutions were obtained for the simple problem.

Both the integrated force method and the stiffness method can handle gross response analysis; however, the classical force method cannot be extended to dynamic and stability analyses of structures.

Versatility of Integrated Force Method

The integrated force method is applicable to static, dynamic, and stability analyses of structures idealized as

(1) Continua (here the analysis utilizes the novel boundary compatibility conditions)

(2) Discrete structures such as finite element models

The IFM has its own variational functional from which the analysis equations for continua and the appropriate internal energy equivalent matrices of finite element analysis can be obtained. The IFM variational functional yields all known equations of structural mechanics along with the additional BCC's. The IFM functional can be specialized to obtain the potential energy and complementary energy functionals. Like the stiffness method, which is known to be a versatile method, the IFM is also a versatile analysis formulation.

Concluding Remarks

The features common to the integrated force (IFM) and stiffness (SM) methods are as follows:

1. Both the IFM and the SM are amenable to computer automation.
2. Both formulations can handle static, dynamic, and stability analyses of continua and finite element discrete structures.
3. Both methods have their own variational functionals.

In IFM all internal forces are obtained from loads in a single step ($[S]\ \{F\} = \{P\}^*$). Displacements are computed from forces by backsubstitution. In the SM displacements are obtained from loads first ($[K]\ \{X\} = \{P\}$); then forces are computed from displacements by backsubstitution.

The IFM bestows appropriate emphasis on equilibrium equations and compatibility conditions. The SM emphasizes the equilibrium equations. In finite element analysis the IFM ensures the satisfaction of element interface compatibility conditions. In contrast, this condition is neglected in the SM and is expected to be satisfied by way of mesh refinements.

Test examples show that the IFM yields accurate responses for both stresses and displacements even for very coarse finite element models. The SM requires a much finer mesh to match IFM accuracy.

The IFM equations are better conditioned than the equations of the stiffness formulation. The IFM governing matrix [S] is much sparser than the stiffness matrix [K]. The IFM requires fewer computations than the SM to generate an accurate solution.

The integrated force method is the true force method. It is free from the concepts of redundants and basic determinate structure, which deterred automation of the classical force method.

Lewis Research Center
National Aeronautics and Space Administration
Cleveland, Ohio, April 7, 1989

Appendix A
Analysis by Integrated Force Method

This appendix is offered here as an elementary introduction to the basic concepts of the integrated force method (IFM). As will be shown, the IFM augments the equilibrium equations for indeterminate structures with constraints on element deformations. These constraints express the requirement that the structural elements fit together after deformations due to external loads. These constraints in the IFM are written in terms of member forces and represent the discretized version of the well-known compatibility conditions of the elasticity theory. This is in contrast to the standard force method (SFM), where the additional conditions imposed are obtained by ad hoc selection of redundants and cuts and then requirements are formulated to close the gaps at the selected cuts.

The essential difference is that the IFM uses global compatibility conditions, whereas the SFM uses selected local conditions of deformation continuity. The SFM was developed in the precomputer era; therefore its goal was to generate and solve a small set of simultaneous equations. When it was interpreted for computer application, three difficulties emerged. One was how to automate the arbitrary selections of the cuts, the second was that the process was more computer intensive than the competing displacement method, and the third was the higher level of difficulty in developing a library of finite elements than in the case of the competing displacement method. The IFM overcomes all these difficulties for the price of an unsymmetrical set of equations, which are, however, computationally less intentive than the symmetrical equations of the displacement method.

First a very simple, perhaps overly simple problem, a fixed bar shown in figure 11, is considered. For this problem the global compatibility conditions simply state that the sum of element deformations vanishes after loading. This constraint on member deformations can be asserted by observation for this problem. The compatibility condition, however, is developed systematically. As a more general illustration a simple truss example follows.

Example 1—Fixed Bar

The IFM analysis process is illustrated by taking the example of a fixed bar subjected to thermomechanical loads. The bar, along with its end conditions and analysis parameters, is depicted in figure 11. The total length of the bar is 3ℓ. It is idealized by three finite elements consisting of a central element and two boundary elements of equal length ℓ. The cross-sectional areas of the boundary elements A_1 are equal; the area of the central element is A_2. The bar is made of steel; its Young's modulus is E; and its coefficient of thermal expansion is α. The bar is subjected to mechanical loads P_1 and P_2 at one-third and two-thirds of its length. The

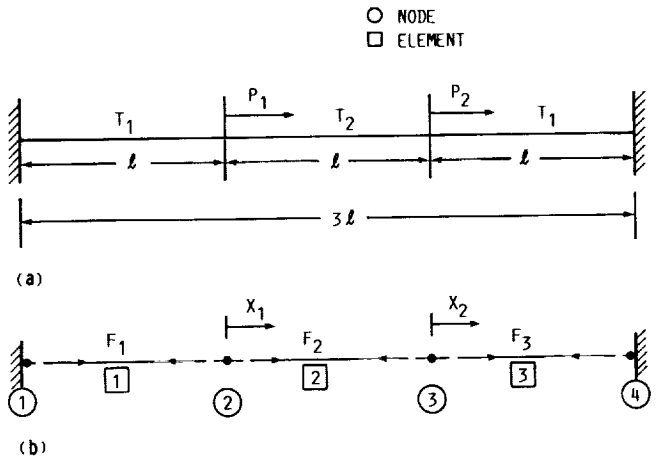

(a) Fixed bar.
(b) Discretized bar (3,2).

Figure 11.—Analysis of bar by integrated force method.

temperature distribution of the central element is T_2. The temperatures of the boundary elements are equal to T_1.

The problem is to determine the forces and the displacements in the bar by the IFM. The structure is discretized by using three elements as shown in figure 11. The force and displacement degrees of freedom of the structure shown in figure 11 are as follows:

(1) Force degrees of freedom: Each element is idealized by one internal force. The bar has three force degrees of freedom (fof = $n = 3$; F_1, F_2, F_3).

(2) Displacement degrees of freedom: The bar has two displacement degrees of freedom, one at each of its two free nodes. Its dof = $m = 2$; X_1, X_2. The bar for the purpose of analysis by the IFM is designated as "bar (3,2)" It has $m = 2$ equilibrium equations and $r = (n-m) = 1$ compatibility condition.

Equilibrium equations.—The two-system equilibrium equations of the bar are assembled from the three elemental equilibrium equations:

Element 1 (refer to fig. 11)

$$[B]^{(1)} = \begin{matrix} 0 \\ 1 \end{matrix} \begin{bmatrix} -1 \\ 1 \end{bmatrix} \qquad \text{(A1)}$$

Element 2

$$[B]^{(2)} = \begin{matrix} 1 \\ 2 \end{matrix} \begin{bmatrix} -1 \\ 1 \end{bmatrix} \qquad \text{(A2)}$$

Element 3

$$[B]^{(3)} = \begin{matrix} 2 \\ 0 \end{matrix} \begin{bmatrix} -1 \\ 1 \end{bmatrix} \tag{A3}$$

The 2×3 system equilibrium matrix $[\beta]$ is obtained by following the standard finite element assembly technique.

$$[B] = \begin{bmatrix} 1 & -1 & 0 \\ 0 & 1 & -1 \end{bmatrix} \tag{A4a}$$

The two equilibrium equations can be written as

$$\begin{bmatrix} 1 & -1 & 0 \\ 0 & 1 & -1 \end{bmatrix} \begin{Bmatrix} F_1 \\ F_2 \\ F_3 \end{Bmatrix} = \begin{Bmatrix} P_1 \\ P_2 \end{Bmatrix} \tag{A4b}$$

Compatibility conditions.—The first step in obtaining the compatibility conditions is to establish the deformation displacement relations $\{\beta\} = [B]^T \{X\}$, refer to eq. (19) of the main text). The deformation vector $\{\beta\}$ of dimension 3×1 corresponds to the three elemental expansions due to forces F_1, F_2, and F_3, respectively. The deformation displacement relation has the following form:

$$\begin{Bmatrix} \beta_1 \\ \beta_2 \\ \beta_3 \end{Bmatrix} = \begin{bmatrix} 1 & 0 \\ -1 & 1 \\ 0 & -1 \end{bmatrix} \begin{Bmatrix} X_1 \\ X_2 \end{Bmatrix} \tag{A5}$$

The two displacements are eliminated from the three DDR's by simple algebra to obtain one ($r = n - m = 3 - 2 = 1$) compatibility condition. The CC in terms of deformations ($[C]\{B\} = \{0\}$) has the following explicit form:

$$\begin{bmatrix} 1 & 1 & 1 \end{bmatrix} \begin{Bmatrix} \beta_1 \\ \beta_2 \\ \beta_3 \end{Bmatrix} = \{0\} \tag{A6}$$

The CC constrains the total elongation of the bars to zero ($\beta_1 + \beta_2 + \beta_3 = 0$), the same as could have been asserted also by observation in this case.

From equation (A6) the compatibility matrix [C] is obtained as

$$[C] = \begin{bmatrix} 1 & 1 & 1 \end{bmatrix} \tag{A7}$$

In order to express the CC given by equation (A7) in terms of forces (refer to eq. (5) of the main text), the flexibility matrix is required. The concatenated flexibility matrix [G] for the structure has the following standard form:

$$[G] = \begin{bmatrix} \dfrac{\ell}{A_1 E} & & \\ & \dfrac{\ell}{A_2 E} & \\ & & \dfrac{\ell}{A_1 E} \end{bmatrix} \tag{A8}$$

Effective initial deformations.—The right side of equation (A6) is zero for the case of mechanical loads. If there are additional prescribed deformations due to some effect (e.g., thermal expansion), they are accommodated in the effective initial deformation vector $\{\delta R\}$ (refer to eq. (1) of the main text). The effective initial deformation vector is obtained from initial deformations $\{\beta\}_0$ and the compatibility matrix [C]. The initial deformation vector has the following form:

$$\begin{Bmatrix} \beta_{10} \\ \beta_{20} \\ \beta_{30} \end{Bmatrix} = \alpha \begin{Bmatrix} T_1 \\ T_2 \\ T_1 \end{Bmatrix} \tag{A9}$$

The effective initial deformation vector $\{\delta R\}$ is obtained from the formula $\{\delta R\} = -[C]\{\beta\}_0$ as

$$\{\delta R\} = -\alpha(2T_1 + T_2) \tag{A10}$$

Take as an example the temperature distributions $T_1 = T_0/2$ and $T_2 = -T_0$. For this temperature profile the effective initial deformation vector $\{\delta R\} = 0$. Since $\{\delta R\}$ is zero, such compatible initial deformations do not induce forces in the structure. This fact was known before the IFM analysis was begun.

From the definition of matrices [B], [C], and [G] the final governing IFM equation ($[S]\{F\} = \{P\}^*$) is assembled as

$$\begin{bmatrix} 1 & -1 & 0 \\ 0 & 1 & -1 \\ 1 & A_1/A_2 & 1 \end{bmatrix} \begin{Bmatrix} F_1 \\ F_2 \\ F_3 \end{Bmatrix} = \begin{Bmatrix} P_1 \\ P_2 \\ \delta R^* \end{Bmatrix} \tag{A11}$$

Solution of equation (A11) yields the forces from which displacements are calculated by backsubstitution (from eq. (2) of the main text).

Numerical results.—The parameters of the example are as follows:

(1) Lengths of the elements: $\ell_1 = \ell_2 = \ell_3 = 10$ in.
(2) Cross-sectional areas: $A_1 = A_3 = 1$ in.^{2}; $A_2 = 2$ in.^{2}
(3) Modulus of elasticity: $E = 30\,000$ ksi
(4) Poisson's ratio: $\nu = 0.3$

Case 1, mechanical loads only.—The pressures are $P_1 = 1000$ kips and $P_2 = 2000$ kips. The internal forces are $F_1 = 1400$ kips, $F_2 = 400$ kips, and $F_3 = -1600$ kips. The nodal displacements are $X_1 = 0.4667$ in. and $X_2 = 0.5333$ in.

Case 2, mechanical and thermal loads.—The mechanical loads are as given for case 1. The thermal loads correspond to the following temperature distribution: $T_1 = 0$, $T_2 = 2000$ °C, and $T_3 = 0$. The internal forces are $F_1 = -40$ kips, $F_2 = -1040$ kips, and $F_3 = -3040$ kips. The nodal displacements are $X_1 = -0.0133$ in. and $X_2 = 1.0133$ in.

Case 3, uniform temperature.—In this case $T_1 = T_2 = T_3 = 2000$ °C. The internal forces are $F_1 = F_2 = F_3 = -3600$ kips. There is no displacement ($X_1 = X_2 = 0$).

Example 2—Five-Bar Truss

Matrix characteristics.—The characteristics of the governing matrices of the IFM and the SM (IFM matrix versus stiffness matrix [K]) are numerically illustrated by taking the example of the five-bar truss shown in figure 12. The design parameters of the bars of the truss shown in figure 12 are as follows: The cross-sectional areas of the five bars are $A_1 = A_3 = A_4 = A_0$ and $A_2 = A_5 = A_0\sqrt{2}$. The lengths of the five bars are $L_1 = L_3 = L_4 = a$ and $L_2 = L_5 = a\sqrt{2}$. The Young's moduli of the five bars are $E_1 = E_2 = E_3 = E_4 = E_5 = E$. The member forces of the five bars are $\langle F_1, F_2, F_3, F_4, F_5\rangle$. The member deformations of the five bars are $\langle \beta_1, \beta_2, \beta_3, \beta_4, \beta_5\rangle$. The displacements of the two free nodes (fig. 12) are $\langle X_1, X_2, X_3, X_4\rangle$. The prescribed load components are $\langle P_1, P_2, P_3, P_4\rangle$. For clarity the matrix characteristics were examined for both determinate and indeterminate problems.

Determinate problem.—A four-bar determinate structure was generated from the indeterminate truss by eliminating the fifth bar. For determinate structures the equilibrium equations represent both necessary and sufficient conditions for stress analysis. There are no compatibility conditions for determinate structures. The IFM governing equations become

$$[S]\{F\} = [B]\{F\} = \{P\}$$

The IFM equations are obtained from the nodal force balance condition between the member forces {F} and the external loads {P} (refer to fig. 12).

$$\begin{bmatrix} 1 & 1/\sqrt{2} & 0 & 0 \\ 0 & 1/\sqrt{2} & 1 & 0 \\ 0 & 0 & 0 & 1 \\ 0 & 0 & -1 & 0 \end{bmatrix} \begin{Bmatrix} F_1 \\ F_2 \\ F_3 \\ F_4 \end{Bmatrix} = \begin{Bmatrix} P_1 \\ P_2 \\ P_3 \\ P_4 \end{Bmatrix} \qquad \text{(A12)}$$

In the displacement method the system equations are assembled from the elemental equations by following standard finite element assembly techniques. The assembled stiffness equation ([K] {X} = {P}) for the problem has the following form:

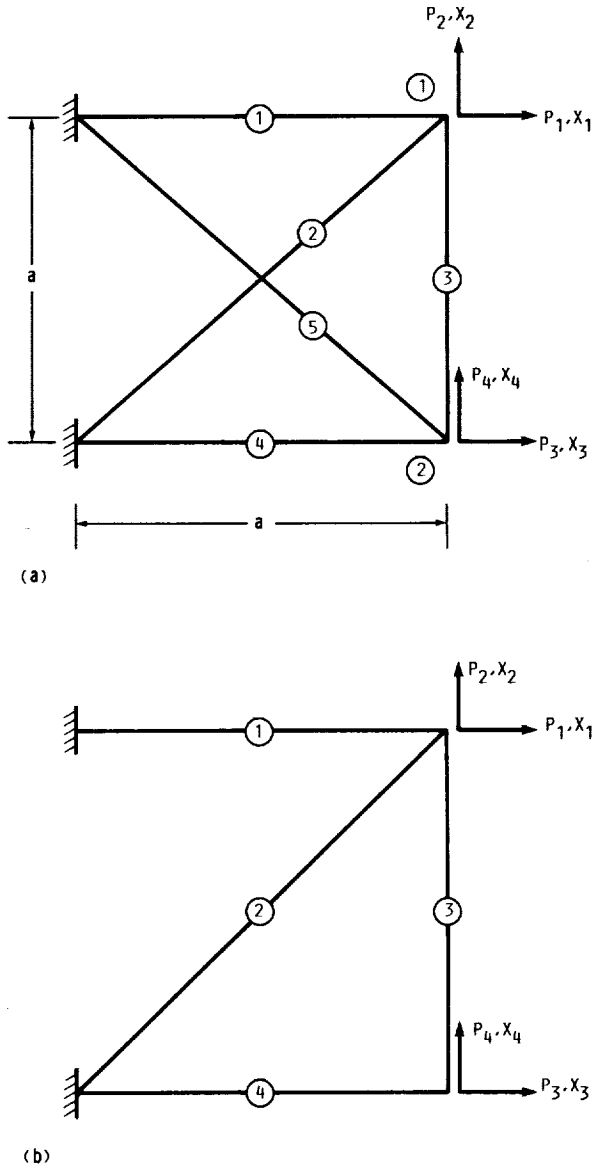

(a) Indeterminate truss (5,4).
(b) Determinate truss (4,4).

Figure 12.—Analysis of truss by integrated force method.

$$\begin{bmatrix} \left(\frac{AE}{L}\right)_1+\left(\frac{AE}{L}\right)_2 & \left(\frac{AE}{L}\right)_2 & 0.0 & 0.0 \\ \left(\frac{AE}{L}\right)_2 & \left(\frac{AE}{L}\right)_2+\left(\frac{AE}{L}\right)_3 & 0.0 & -\left(\frac{AE}{L}\right)_3 \\ 0.0 & 0.0 & \left(\frac{AE}{L}\right)_4 & 0.0 \\ 0.0 & -\left(\frac{AE}{L}\right)_3 & 0.0 & \left(\frac{AE}{L}\right)_3 \end{bmatrix} \begin{Bmatrix} X_1 \\ X_2 \\ X_3 \\ X_4 \end{Bmatrix} = \begin{Bmatrix} P_1 \\ P_2 \\ P_3 \\ P_4 \end{Bmatrix} \tag{A13}$$

From the IFM matrix [S] (eq. (A12)) and the stiffness matrix [K] (eq. (A13)) we made the following observations:

(1) Both are square matrices of dimension 4×4.

(2) The matrix [S] for the determinate truss is a triangular matrix. For general determinate structures irrespective of their complexity, the governing matrix [S] after some rearrangement of rows and columns can be represented as a triangular matrix. The stiffness matrix [K] is not a triangular matrix for determinate systems as can be seen even for this trivial example. The triangular system of equations requires insignificant computation, and it can be solved even manually irrespective of the size or complexity of the problem. This feature of the force method made it the popular analytical method in the precomputer era. The classical force method utilizes this property of the governing matrix even for indeterminate structures and reduces the number of simultaneous equations to the order of only the redundants.

(3) The coefficients of matrix [S] tend to be of the same order of magnitude, and they are dimensionless numbers. These two features of the matrix ensure that matrix [S] is numerically stable.

The coefficients of the stiffness matrix have the dimensions of force per unit length. Since the coefficients depend on material properties and design parameters, an ill-conditioned stiffness matrix can be easily obtained by changing those properties.

For this simple example or any other complex determinate system the force method should be followed in analyses for the following reasons:

(1) The most important variables, namely forces, required by design engineers are obtained directly in the force method.

(2) The force method requires little computation; unlike for the displacement method there are no simultaneous equations to solve.

(3) Its equations are well conditioned.

From forces {F} the required number of displacements can be obtained in a small fraction of the total analysis time. It is inefficient to use the stiffness method or any other formulation for the stress analysis of determinate problems.

Compatibility conditions for determinate structures.— Determinate structures do not have any compatibility conditions (CC's). This fact is numerically illustrated by the example of the determinate truss. Generation of CC's for a determinate system can be attempted by following the two-step procedure given in the text in the section "Generation of Compatibility Matrix [C]." In the first step the DDR's are established. In the second step the CC's are generated from the DDR's by eliminating the displacements.

The DDR's of the determinate structure can be obtained by using the equilibrium matrix $[\beta]$ as $\{\beta\} = [B]^T \{X\}$. The DDR's for the determinate truss have the following form:

$$\begin{Bmatrix} \beta_1 \\ \beta_2 \\ \beta_3 \\ \beta_4 \end{Bmatrix} = \begin{bmatrix} 1 & 0 & 0 & 0 \\ 1/\sqrt{2} & 1/\sqrt{2} & 0 & 0 \\ 0 & 1 & 0 & -1 \\ 0 & 0 & 1 & 0 \end{bmatrix} \begin{Bmatrix} X_1 \\ X_2 \\ X_3 \\ X_4 \end{Bmatrix} \tag{A14}$$

In equation (A14) the bar deformations (elongations or contractions) are represented by (β_1, β_2, β_3, and β_4). The four deformations can be uniquely determined in terms of the four displacements as a solution to equation (A14). In other words there is no constraint on deformations, and as a result determinate structures do not have any compatibility conditions.

Indeterminate problem.—The IFM equilibrium equations (EE's) for the five-bar indeterminate truss can be written as

$$\begin{bmatrix} 1 & 1/\sqrt{2} & 0 & 0 & 0 \\ 0 & 1/\sqrt{2} & 1 & 1 & 0 \\ 0 & 0 & 0 & 0 & 1/\sqrt{2} \\ 0 & 0 & -1 & -1 & -1/\sqrt{2} \end{bmatrix} \begin{Bmatrix} F_1 \\ F_2 \\ F_3 \\ F_4 \end{Bmatrix} = \begin{Bmatrix} P_1 \\ P_2 \\ P_3 \\ P_4 \end{Bmatrix} \tag{A15}$$

The EE's of the indeterminate problem given by equation (A15) still contain a triangular factor (as was the case for determinate structures). However, there are fewer EE's than unknowns, since there are four simultaneous equations and five unknown forces. Equation (A15) cannot be solved for the five unknown forces, hence the indeterminancy. An additional equation is required to augment the system to five equations in five unknowns, which can be solved for the five member forces. This additional equation is the compatibility condition.

The CC to augment the 4×5 EE for the truss is obtained in two steps. In the first step the CC in deformations is generated from the DDR. In the next step the CC in deformations is written in forces by using the constitutive relations.

The DDR for the five-bar truss has the following form:

$$\begin{Bmatrix} \beta_1 \\ \beta_2 \\ \beta_3 \\ \beta_4 \\ \beta_5 \end{Bmatrix} = \begin{bmatrix} 1 & 0 & 0 & 0 \\ 1/\sqrt{2} & 1/\sqrt{2} & 0 & 0 \\ 0 & 1 & 0 & -1 \\ 0 & 0 & 1 & 0 \\ 0 & 0 & 1/\sqrt{2} & -1/\sqrt{2} \end{bmatrix} \begin{Bmatrix} X_1 \\ X_2 \\ X_3 \\ X_4 \end{Bmatrix} \quad \text{(A16)}$$

In equation (A16) five deformations are expressed in terms of four displacements: thus there is a single ($n - m = 5 - 4 = 1$) constraint on deformations that represent the CC. The CC is obtained by eliminating the four displacements (X_1, X_2, X_3, and X_4) from the five DDR's given by equation (A16). The CC has the following explicit form:

$$\begin{bmatrix} 1 & -\sqrt{2} & 1 & 1 & -\sqrt{2} \end{bmatrix} \begin{Bmatrix} \beta_1 \\ \beta_2 \\ \beta_3 \\ \beta_4 \\ \beta_5 \end{Bmatrix} = \{0\} \quad \text{(A17)}$$

The CC (eq. (A17)) of deformations is expressed in terms of forces by using the force deformation relations of the truss. These relations ($\{\beta\} = [G]\{F\}$) can be written in matrix notation as

$$\begin{Bmatrix} \beta_1 \\ \beta_2 \\ \beta_3 \\ \beta_4 \\ \beta_5 \end{Bmatrix} = \begin{bmatrix} (L/AE)_1 & 0.0 & 0.0 & 0.0 & 0.0 \\ 0.0 & (L/AE)_2 & 0.0 & 0.0 & 0.0 \\ 0.0 & 0.0 & (L/AE)_3 & 0.0 & 0.0 \\ 0.0 & 0.0 & 0.0 & (L/AE)_4 & 0.0 \\ 0.0 & 0.0 & 0.0 & 0.0 & (L/AE)_5 \end{bmatrix} \begin{Bmatrix} F_1 \\ F_2 \\ F_3 \\ F_4 \\ F_5 \end{Bmatrix}$$

(A18)

Equations (A17) and (A18) normalized with respect to the flexibility parameter L/AE yield the CC of the integrated force method expressed in terms of force variables as

$$\begin{bmatrix} 1 & -\sqrt{2} & 1 & 1 & -\sqrt{2} \end{bmatrix} \begin{Bmatrix} F_1 \\ F_2 \\ F_3 \\ F_4 \\ F_5 \end{Bmatrix} = \{0\} \quad \text{(A19)}$$

The CC given by equation (A19) is added to the EE given by equation (A15) to obtain the governing IFM equation ($[S]\{F\} = \{P\}^*$) as

$$\begin{bmatrix} 1 & 1/\sqrt{2} & 0 & 0 & 0 \\ 0 & 1/\sqrt{2} & 1 & 0 & 0 \\ 0 & 0 & 0 & 1 & 1/\sqrt{2} \\ 0 & 0 & -1 & 0 & -1/\sqrt{2} \\ 1 & -\sqrt{2} & 1 & 1 & -\sqrt{2} \end{bmatrix} \begin{bmatrix} F_1 \\ F_2 \\ F_3 \\ F_4 \\ F_5 \end{bmatrix} = \begin{bmatrix} P_1 \\ P_2 \\ P_3 \\ P_4 \\ 0 \end{bmatrix} \quad \text{(A20)}$$

Solution of equation (A20) of dimension 5×5 yields the five member forces F_1, F_2, F_3, F_4, and F_5.

The governing equation of the stiffness method ($[K]\{X\} = \{P\}$) for the five-bar truss has the following form:

$$\begin{bmatrix} \left(\frac{AE}{L}\right)_1 + \left(\frac{AE}{L}\right)_2 & \left(\frac{AE}{L}\right)_2 & 0.0 & 0.0 \\ \left(\frac{AE}{L}\right)_2 & \left(\frac{AE}{L}\right)_2 + \left(\frac{AE}{L}\right)_3 & 0.0 & -\left(\frac{AE}{L}\right)_3 \\ 0.0 & 0.0 & \left(\frac{AE}{L}\right)_4 + \left(\frac{AE}{L}\right)_5 & -\left(\frac{AE}{L}\right)_5 \\ 0.0 & -\left(\frac{AE}{L}\right)_3 & -\left(\frac{AE}{L}\right)_5 & \left(\frac{AE}{L}\right)_3 + \left(\frac{AE}{L}\right)_5 \end{bmatrix} \begin{Bmatrix} X_1 \\ X_2 \\ X_3 \\ X_4 \end{Bmatrix} = \begin{Bmatrix} P_1 \\ P_2 \\ P_3 \\ P_4 \end{Bmatrix}$$

(A21)

The solution of equation (A21) yields the nodal displacements.

The three conclusions for determinate structures stated earlier hold true even for indeterminate structures with the following exceptions:

(1) The IFM yields $n \times n$ (here 5×5) equations where the dimension of the stiffness equation is $m \times m$ (here 4×4).

(2) The triangular factor of matrix [S] is disturbed because of the compatibility conditions.

It is common observation that

(1) In the stiffness method compatibility is presumed to be satisfied apriori by appropriate choice of displacement fields, and the equilibrium equations ($[K]\{X\} = \{P\}$) are the governing equations.

(2) In the classical force method (Airy's stress function formulation being the typical example) the equilibrium is satisfied apriori (by suitable assumptions on stresses) and the CC's are the governing equations.

The question is, among EE and CC which one is assumed and which one is enforced in the integrated force method? In the analysis of indeterminate structures (refer to IFM governing equation $[S]\{F\} = \{P\}^*$ (eq. (A20) for the indeterminate truss) both the EE's and the CC's are simultaneously and explicitly enforced by the integrated force method. It can be verified that among the five available methods of structural analysis, (1) the classical Airy force method, (2) the stiffness method, (3) the mixed method, (4) the total formulation, and (5) the integrated force method, only the integrated force method enforces both EE's and CC's simultaneously.

The primary IFM variables are the forces, not a combination of forces, displacements, and deformations. Therefore the integrated force method is a direct formulation, and it should not be confused with the mixed method (in which forces and displacements are considered as $m + n$ simultaneous primary unknowns) or with the total formulation (in which forces, deformations, and displacements are treated as the $m + 2n$ primary unknowns).

Appendix B
Symbols

A_1, A_2, A_3	cross-sectional areas of three truss bars
a, b	dimension of rectangular element
[B]	equilibrium matrix
$[B]_P$	Prezemieniecki's equilibrium matrix
$[B]_R$	Robinson's equilibrium matrix
$[B]_s, [B]_a$	IFM equilibrium matrices
[C]	compatibility matrix
[D]	damping matrix
$[D]_f$	IFM damping matrix
E	Young's modulus
e	eigen ratio
F	internal force
{F}	force vector of dimension n
$\{F\}_m$	force mode shape of dimension n
f	frequency
[G]	flexibility matrix of dimension $(n \times n)$
$[G]_e$	element flexibility matrix
H_{ij}	Hermite polynomials $(i,j = 0, 1, 2)$
h	plate thickness
i	imaginary unity
[J]	deformation coefficient matrix of dimension $(m \times m)$
[K]	stiffness matrix of dimension $(m \times m)$
$[K]_g$	geometric stiffness matrix of dimension $(m \times n)$
L, ℓ	length parameters
$L_1 \ldots L_5$	lengths of five bars
M_x, M_y, M_{xy}	plate bending moments
[M]	mass matrix of dimension $(m \times m)$
$[M]_f$	IFM mass matrix
m	displacement degrees of freedom
m_0	lumped mass
N_x, N_y, N_{xy}	membrane stress resultants
n	force degrees of freedom
n_x, n_y	direction cosines
{P}	mechanical load vector of dimension m
$\{P\}^i$	equivalent loads due to initial imperfections
$\{P\}^*$	IFM load vector of dimension n
r	number of compatibility conditions, $r = n - m$
[S]	IFM governing matrix of dimension $(n \times n)$
$[S]_b$	IFM stability matrix
t	time parameter
U_c	complementary strain energy
U_p	strain energy
u, v	membrane displacement components
w	transverse displacement
w_c	transverse displacement at center
$X_1, X_2, \ldots, X_{12}$	displacement variables
{X}	displacement vector of dimension m
$\{X\}_m$	displacement mode shape of dimension m
x, y, z	Cartesian coordinates
α	coefficient of thermal expansion
$\{\beta\}$	deformation vector of dimension n
β_K	K^{th} deformation component
$\{\beta\}_0$	initial deformation vector
γ	shear strain
$\{\delta R\}$	effective initial deformation vector
δ_R	residue in BCC
$(\epsilon_x, \epsilon_y, \gamma_{xy})$	strain components
θ_x, θ_y	rotation about x and y axes
λ	eigenvalue
ν	Poisson's ratio
ω	radian frequency

Subscripts:

crt	critical load
max, min	maximum or minimum values

Superscript:

T	transpose of matrix or vector

References

1. Patnaik, S.N.: Integrated Force Method Versus the Standard Force Method. Comput. Struct., vol. 22, no. 2, 1986, pp. 151–163.
2. Patnaik, S.N.: An Integrated Force Method for Discrete Analysis. Int. J. Numer. Methods Eng., vol. 6, no. 2, 1973, pp. 237–251.
3. Love, A.E.H.: A Treatise on the Mathematical Theory of Elasticity, Dover, New York, 1944.
4. McGuire, W.; and Gallagher, R.H.: Matrix Structural Analysis. Wiley, New York, 1979.
5. Gallagher, R.H.; Rattinger, I.; and Archer, J.S.: A Correlation Study of Methods of Matrix Structural Analysis. Agardograph 69, The MacMillan Co., New York, 1964.
6. Timoshenko, S.: History of Strengths of Material. McGraw-Hill, New York, 1953.
7. Patnaik, S.N.: The Variational Energy Formulation for the Integrated Force Method. AIAA J., vol. 24, no. 1, Jan. 1986, pp. 129–137.
8. Whipple, S.: A Work on Bridge Building. Utica, New York, 1847.
9. Stress Recovery at Grid Points, MSC/NASTRAN Applications Manual, MacNeal-Schwendler Corporation, Los Angeles, CA, 1982, Section 2.2.
10. Patnaik, S.N.; and Yadagiri, S.: Frequency Analysis of Structures by Integrated Force Method. J. Sound Vibration, vol. 83, no. 1, July 8, 1982, pp. 93–109.
11. Patnaik, S.N.; and Joseph, K.T.: Compatibility Conditions From Deformation Displacement Relationship. AIAA J., vol. 23, no. 8, Aug. 1985, pp. 1291–1293.
12. Patnaik, S.N.; and Joseph, K.T.: Generation of the Compatibility Matrix in the Integrated Force Method. Comput. Methods Appl. Mech. Eng., vol. 55, no. 3, May 1986, pp. 239–257.
13. Patnaik, S.N.; and Yadagiri, S.: Design for Frequency by the Integrated Force Method. Comput. Methods Appl. Mech. Eng., vol. 16, no. 2, Nov. 1978, pp. 213–230.
14. Patnaik, S.N.; and Gallagher, R.H.: Gradients of Behaviour Constraints and Reanalysis via the Integrated Force Method. Int. J. Numer. Methods Eng., vol. 23, no. 12, 1986, pp. 2205–2212.
15. Patnaik, S.N.; and Nagaraj, M.S.: Analysis of Continuum by the Integrated Force Method. Computers Structures, vol. 26, no. 6, 1987, pp. 899–905.
16. Vijayakumar, K.; Krishna Murty, A.V.; and Patnaik, S.N.: A Basis for the Analysis of Solid Continua Using the Integrated Force Method. AIAA J., vol. 26, no. 5, May 1988, pp. 628–629.
17. Przemieniecki, J.S.: Theory of Matrix Structural Analysis. McGraw-Hill, New York, 1968.
18. Robinson, J.: Integrated Theory of Finite Element Methods. Wiley, New York, 1973.
19. Gallagher, R.H.: Finite Element Analysis: Fundamentals. Prentice-Hall, 1975.
20. Timoshenko, S.: Theory of Plates and Shells. McGraw-Hill, New York, 1959.
21. Argyris, J.H.: Energy Theorems and Structural Analysis. Butterworth Scientific Publications, London, 1960.
22. Argyris, J.H.; and Kelsey, S.: The Matrix Force Method of Structural Analysis With Some New Applications to Aircraft Wings. ARC-R&M-3034, Aeronautical Research Council, London, Feb. 1956.
23. Argyris, J.H.: ASKA—Automatic System for Kinematic Analysis. Nucl. Eng. Des., vol. 10, no. 4, Aug. 1969, pp. 441–455.
24. MSC/NASTRAN—NASA Structural Analysis. The MacNeal-Schwendler Corp., Los Angeles, CA, 1981.
25. MacNeal R.H.; and Harder, R.L.: A Proposed Standard Set of Problems to Test Finite Element Accuracy. Finite Elements in Analysis and Design, vol. 1, no. 1, Apr. 1985, pp. 3–20.
26. Reid, J.K.: Fortran Subroutines for Handling Sparse Linear Programming Bases. Report AERE-R-8269, Atomic Energy Research Establishment, 1976.
27. Robinson, J.: Automatic Selection of Redundancies in the Matrix Force Method: The Rank Technique. Canadian Aeronautical J., vol. 11, no. 1, Jan. 1965, pp. 9–12.
28. Przemieniecki, J.S.; and Denke, P.H.: Joining of Complex Sub-Structures by the Matrix Force Method. J. Aircraft, vol. 3, no. 3, May-June 1966, pp. 236–243.
29. Kaneko, I.; Lawo, M.; and Thierauf, G.: On Computational Procedures for Force Method. Int. J. Numer. Methods Eng., vol. 18, no. 10, 1982, pp. 1469–1495.
30. Plemmons, R.J.: A Parallel Block Iterative Scheme Applied to Computations in Structural Analysis. SIAM J. Algebraic Discrete Methods, vol. 7, no. 3, 1986, pp. 337–347.
31. Heath, M.T.; Plemmons, R.J.; and Ward, R.C.: Sparse Orthogonal Schemes for Structural Optimization Using the Force Method. SIAM J. Sci. Stat. Comput., vol. 15, no. 3, Sept. 1984, pp. 514–532.
32. Berke, L.: Optimality Criteria Using a Force Method Analysis Approach. Foundations of Structural Optimization: A Unified Approach, A.J. Morris, ed., John Wiley & Sons, New York, 1982, pp. 237–269.
33. Fraeijs de Veubeke, B.: Displacement and Equilibrium Models in the Finite Element Method. Stress Analysis, O.C. Zienkiewicz and G.S. Holister, eds., John Wiley & Sons, New York, 1965, pp. 145–197.

NASA
National Aeronautics and Space Administration

Report Documentation Page

1. Report No.	2. Government Accession No.	3. Recipient's Catalog No.
NASA TP-2937		

4. Title and Subtitle
Integrated Force Method Versus Displacement Method for Finite Element Analysis

5. Report Date
February 1990

6. Performing Organization Code

7. Author(s)
Surya N. Patnaik, Laszlo Berke, and Richard H. Gallagher

8. Performing Organization Report No.
E-4604

10. Work Unit No.
505-63-1B

9. Performing Organization Name and Address
National Aeronautics and Space Administration
Lewis Research Center
Cleveland, Ohio 44135-3191

11. Contract or Grant No.

13. Type of Report and Period Covered
Technical Paper

12. Sponsoring Agency Name and Address
National Aeronautics and Space Administration
Washington, D.C. 20546-0001

14. Sponsoring Agency Code

15. Supplementary Notes
Surya N. Patnaik, National Research Council-NASA Research Associate; Laszlo Berke, Lewis Research Center; Richard H. Gallagher, Clarkson University, Potsdam, New York 13676.

16. Abstract

A novel formulation termed "the integrated force method" (IFM) has been developed in recent years for analyzing structures. In this method all the internal forces are taken as independent variables, and the system equilibrium equations (EE's) are integrated with the global compatibility conditions (CC's) to form the governing set of equations. In IFM the CC's are obtained from the strain formulation of St. Venant, and no choices of redundant load systems have to be made, in constrast to the standard force method (SFM). This property of IFM allows the generation of the governing equation to be automated straightforwardly, as it is in the popular stiffness method (SM). In this report IFM and SM are compared relative to the structure of their respective equations, their conditioning, required solution methods, overall computational requirements, and convergence properties as these factors influence the accuracy of the results. Overall, this new version of the force method produces more accurate results than the stiffness method for comparable computational cost.

17. Key Words (Suggested by Author(s))	18. Distribution Statement
Finite elements; Integrated force method; Stiffness method; Flexibility; Compatibility	Unclassified – Unlimited Subject Category 39

19. Security Classif. (of this report)	20. Security Classif. (of this page)	21. No of pages	22. Price*
Unclassified	Unclassified	36	A03

NASA FORM 1626 OCT 86

*For sale by the National Technical Information Service, Springfield, Virginia 22161

NASA-Langley, 1990